Bank of England

Persistent and transitory inflation in the euro area: insights from global and domestic shocks

Staff Working Paper No. 1,170
February 2026

Clemente Pinilla-Torremocha

Bank of England

Staff Working Paper No. 1,170

Persistent and transitory inflation in the euro area: insights from global and domestic shocks

Clemente Pinilla-Torremocha[1]

Abstract

This paper investigates the post-Covid inflation surge in the euro area, combining three features: decomposition of long-term trends and business-cycle dynamics – such as potential GDP, trend inflation, output-gap, and inflation-gap; time-varying volatility and fat-tailed distributions to accommodate extreme observations; and structural shock identification, distinguishing shocks by their persistence (permanent versus transitory) and domain (global versus domestic, demand versus supply, or energy specific). Unlike the existing literature, findings show that domestic supply shocks feed into the persistent component of euro-area inflation, raising trend inflation to 3% by 2022. Demand shocks – domestic and global – manifest in the transitory component (inflation gap), explaining 85% of the post-Covid inflation surge.

Key words: Inflation dynamics, trends and cycles, permanent and transitory shocks, stochastic volatility, fat-tails, domestic-global, demand-supply.

JEL classification: E31, E32, E44.

---

(1) Bank of England and European Research University, London.
Email: clemente.pinillatorremocha@bankofengland.co.uk

The views expressed in this paper are those of the authors and do not necessarily represent the views of the Bank of England. This paper previously circulated under the title ‘Stable, missing and wild inflation: The case of the euro area’. This paper is a revised version of one of the chapters of my PhD dissertation produced at Universidad de Alicante. I am grateful to Professor Gabriel Pérez-Quirós for his guidance and advice. This paper has also benefited from the insightful comments of Beatriz de Blas, Joan Paredes, Iván Payá, and Marta García-Rodríguez. I thank all the professors at the Alicante Macroeconomic PhD Workshop, and participants at ASSET 2023, SAEe 2024, IAAE 2024, and ESEM 2024. I acknowledge the financial support from the Universidad de Alicante and the receipt of a full fee waiver for the SAEe 2024 – 48th Simposio.

The Bank’s working paper series can be found at www.bankofengland.co.uk/working-paper/staff-working-papers

Bank of England, Threadneedle Street, London, EC2R 8AH
Email: enquiries@bankofengland.co.uk

ISSN 1749-9135 (on-line)

1. Introduction

For years, inflation in the euro area had remained subdued, until the post pandemic episode when it surged to levels not observed in four decades. This study emerges in the context of a complex economic crisis triggered by the COVID-19 pandemic, marked by a sequence of global and domestic shocks—supply chain disruptions, expansive fiscal and monetary stimulus during the reopening phase, and a global energy supply shock following the Russian invasion of Ukraine.

This paper addresses two central questions: (1) What are the structural channels driving euro area (EA) inflation? This is examined through the lens of both global and domestic shocks, further disaggregated into demand and supply components. While many economists agree that the imbalance between aggregate demand and supply contributed to the initial surge in inflation, there remains considerable debate over the relative importance of domestic versus global forces. (2) Do these structural channels primarily affect the transitory component of inflation—the inflation gap—or the persistent component—trend inflation? This decomposition is both novel and policy-relevant, as it helps distinguish inflationary pressures reflecting persistent changes in economic conditions from those driven by more temporary disturbances—an essential input for the design of monetary policy.

I organize the narrative around three episodes: the long phase of inflation broadly anchored around 2%, the "missing inflation" period (2012–2017), and the post-COVID inflation surge. This framing also speaks to the renewed debate on the anchoring of expectations at 2%—first challenged from below during the sovereign-debt-crisis, and more recently from above after 2020.[1]

The approach adopted here builds on and integrates two key methodologies commonly used to study inflation dynamics within a unified framework. The first involves identifying the structural drivers of observed inflation—emphasizing global channels, supply bottlenecks and energy-related in some contributions Ciccarelli and García (2021); Ascari et al. (2024a); Arce et al. (2024) and demand-side (including fiscal) forces in others Giannone and Primiceri (2024); Ascari et al. (2024b). Yet this literature typically interprets inflation fluctuations around a deterministic component and, crucially for the present question, does not assess whether these channels operate through the persistent component of inflation (trend), the transitory component (inflation gap), or both. This paper takes that distinction as central.

The second approach involves estimating an unobserved components trend-cycle model. For example, Jarociński and Lenza (2018) found that trend inflation in the EA remained stable near 2% from 2000 to 2016, attributing the "missing inflation" to negative transitory developments. However, their analysis did not explore the structural sources underlying movements in trend inflation or the inflation gap. This paper bridges that gap in a unified framework that

[1] This debate has been ongoing in both academic and policy circles since inflation remained persistently below 2% after 2012, despite expectations of a rise in inflation due to the ongoing recovery. Notably, the average headline inflation in the euro area from 2012Q1 to 2018Q4 was just 1.28%. In contrast, current inflation dynamics may represent a paradigm shift.

decomposes inflation into trend and gap components and identifies the structural shocks driving each.

The empirical framework combines three key components. First, following Del Negro et al. (2017, 2019), the model decomposes macroeconomic variables into long-term and business-cycle components—trend inflation and potential GDP versus the inflation gap and output gap.[2] Second, it incorporates time-varying volatility and fat-tailed innovations to accommodate episodes of extreme volatility—most notably the COVID-19 period.[3][4] Third, the model identifies structural shocks along two dimensions: persistence (permanent versus transitory) and domain (global versus domestic; demand versus supply; energy-specific). The identification strategy relies on sign and magnitude restrictions. In line with standard macroeconomic theory, supply-side shocks are characterized by opposite movements in output and inflation, while demand-side shocks induce a positive comovement, as in Canova and De Nicolo (2002). The identification of energy supply shocks draws on the findings of Kilian (2008, 2009). To distinguish between domestic and global shocks, I adopt the methodology of Corsetti, Dedola and Leduc (2014), which assumes that global shocks have a stronger effect on global variables than on domestic ones, and vice versa.[5]

I document the following findings: (1) Post-COVID EA inflation surge: Following the post-COVID economic reopening, trend inflation in the euro area rose above the 2% level, reaching approximately 3% by 2022Q2. This increase was predominantly driven by supply shocks, particularly domestic supply, which fed into the persistent component of inflation. Notably, the majority of the increase in EA inflation is attributable to the inflation gap, accounting for 85% of the total rise. This component is primarily explained by demand shocks—both domestic and global. Although recent trend inflation dynamics are not yet extensively documented in the literature, they align with the ECB's revised monetary policy strategy. By the end of 2022, the ECB adjusted its stance on inflation, shifting from the view that *'the current inflation spike is temporary and driven largely by transitory factors'* in 2021Q4, to *'[...] inflation is expected to decline from an average of 8.4% in 2022, 6.3% in 2023, 3.4% in 2024, and 2.3% in 2025'* by 2022Q4.

(2) Trend inflation fluctuations prior to COVID: The EA trend inflation has experienced two significant declines: the first in the 1990s, when it decreased from 4% to 2% and remained anchored at that level for nearly two decades; and the second between 2012Q3 and 2016Q1,

[2]Seminal contributions to the trend-cycle literature began with the univariate models of Beveridge and Nelson (1981), Harvey (1985), Watson (1986), and Clark (1987). In the 2000s, Stock and Watson (2007) extended these models by incorporating stochastic volatility into a univariate unobserved component trend-cycle framework.

[3]My model extends the VAR with common trends in Del Negro et al. (2017, 2019) by allowing for stochastic volatility and fat tails, as in Jacquier et al. (2004).

[4]Related treatments of COVID-19 outliers in VARs include Carriero et al. (2021); Lenza and Primiceri (2022); Schorfheide and Song (2021). As discussed in Section 3, both stochastic volatility and Student's t errors are needed: SV alone can impose overly tight prior beliefs on variance changes in trend components, while t errors reduce spurious SV "compensation" for sharp volatility spikes when separating trends from cycles.

[5]Global shocks are identified using international measures, consistent with the open-economy perspective on inflation dynamics as in Martínez-García and Wynne (2010), Kabukçuoğlu and Martínez-García (2018), and Duncan and Martínez-García (2023).

during which it dropped from 2% to 1%. While the first decline is primarily associated with domestic supply factors, the decline in trend inflation from 2012 to 2016 aligns more closely with the demand-side narrative—both domestic and global—highlighted by Ciccarelli et al. (2017). However, I find this demand-driven effect to primarily impact the persistent component of inflation. Importantly, the estimated EA trend inflation exhibits similar comovement (pre- and post-COVID) with inflation swaps at five-, ten-, and twenty-year horizons.[6]

(3) Second moments and potential GDP: Modeling time-varying volatility (and fat tails) sharpens the trend–cycle split in extreme episodes. In a homoskedastic specification, the COVID-19 GDP collapse is partly absorbed by the output trend, mechanically overstating the decline in potential output; whereas in the baseline specification with stochastic volatility, the collapse is treated as an episodic transitory disturbance and is allocated primarily to the output gap, yielding a more stable and interpretable measure of potential GDP.[7] Additionally, the baseline model implies a marked slowdown in euro area potential GDP growth, from 0.50% q-o-q (early 1990s–2005/06) to 0.24% since 2006. This deceleration is primarily driven by global factors, including both demand and supply shocks, aligning with theories of a persistent shift in globalization following the synchronized collapse of global trade in late 2008 (Baldwin, 2009; Levchenko et al., 2010; Alessandria et al., 2010; Chor and Manova, 2012). Finally, consistent with Giannone and Primiceri (2025), the model identifies strong post-pandemic demand; in the decomposition, domestic demand shocks through 2022 and global demand shocks from 2023 onward contribute positively to the estimated potential GDP.

Related Literature. The recent surge in inflation has become an active area of research, with several studies centering their analysis on the distinction between demand and supply factors. I extend this work by identifying structural drivers—domestic (demand and supply), global (demand and supply), and energy supply—while simultaneously assessing their effects on both the persistent (trend) and transitory (gap) components of inflation.

Given the extensive body of literature on inflation processes, this paper does not aim to provide an exhaustive survey. Rather, it seeks to situate itself within the most relevant strands of the literature, emphasizing its specific contribution in the context of the euro area.

Much of the existing literature relies on structural models—typically Vector Autoregressive (VAR) frameworks—that assess macroeconomic dynamics relative to a deterministic component. Several studies use these frameworks to study the historical drivers of inflation before COVID-19. For instance, Ferroni and Mojon (2014) emphasize global demand shocks, attributing much of the 2008 inflation rise and subsequent decline to these factors. Similarly, Conti et al. (2017) identify a mix of domestic and global demand shocks in 2008–09, and highlight energy supply and domestic demand shocks during the "missing inflation" episode. Ciccarelli et al. (2017) distinguish two stages in the prolonged low-inflation period: an initial stage driven by domestic shocks, followed by one dominated by global shocks. Bobeica and Jarociński (2019)

[6] See Figure 11 in Appendix C.
[7] See Figure 13 in Appendix C.

also stress global demand in 2008, while attributing "missing inflation" primarily to domestic shocks. In contrast, my findings suggest that "missing inflation" in the EA is driven mainly by demand-side shocks—both domestic and global—which reduced trend inflation from 2% to 1%, while supply shocks are the main drivers of the inflation gap during this period.

Regarding more recent inflation dynamics, Ciccarelli and García (2021) ask whether rising U.S. inflation in mid-2021 signaled a return of global inflation, and document a global inflation channel—operating through inflation-compensation markets—that amplifies spillovers from the U.S. to the euro area. Ascari et al. (2024a) and Dao et al. (2024), together with recent *ECB* reports and related studies Arce et al. (2024); Banbura et al. (2023); De Santis (2024) emphasize global supply bottlenecks, supply-chain disruptions, and energy prices as the dominant drivers in 2022.[8] In contrast, other contributions stress demand-side forces Giannone and Primiceri (2024); Ascari et al. (2023); Bergholt et al. (2024a), with Ascari et al. (2024b) highlighting an important role for fiscal shocks. My findings reconcile these views: domestic supply shocks primarily feed into the persistent component, raising trend inflation from 2% to 3%, while domestic and global demand shocks account for most of the rise in the transitory component. Importantly, as emphasized by Bergholt et al. (2024a), not incorporating informative priors on the deterministic component in standard BVARs can significantly affect historical decomposition analyses. In my model, the priors on the stochastic trend of inflation are structured to mitigate such estimation uncertainty.

Much of the euro area literature studies the (de-)anchoring of inflation expectations to explain the "missing inflation" phase and, more recently, the post-COVID surge, but a key challenge is measuring medium- to long-run expectations. Studies use different sources—market-based inflation swaps Strohsal and Winkelmann (2015); Gimeno and Ortega (2016); Hilscher et al. (2022), professional forecasts Jarociński and Lenza (2018); Corsello et al. (2021); Dovern et al. (2020), or both professional and consumer expectations Łyziak and Paloviita (2017)—and reach divergent conclusions (e.g., Gimeno and Ortega (2016) find a decline below 2% from late 2014, while Jarociński and Lenza (2018) report stable trend inflation around 2% over 2000–2016). Relative to this work, I estimate trend inflation using households' perceived inflation and unit labor costs (as a proxy for firms' price-setting expectations), combined with weakly informative priors on the expected volatility of trend inflation. As external validation, I show that the estimated trend comoves with market-based inflation compensation at 5-, 10-, and 20-year horizons—series not used in estimation. This paper aligns with the view of a gradual de-anchoring starting in 2012, and supports a post-COVID rise in trend inflation above 2%, consistent with Hilscher et al. (2022), who highlight heightened risks of persistent inflation in 2022.

The studies closest to this paper in model structure and identification are Johannsen and Mertens (2021), Ascari and Fosso (2024), and Maffei-Faccioli (2025). Johannsen and Mertens (2021) employs a similar model structure to identify U.S. monetary policy shocks from the cyclical component of the policy interest rate and using a recursive point-identification scheme.

[8] Also, see Gonçalves and Koester (2022); O'Brien et al. (2021); Koester et al. (2021, 2022); ECB (2022).

In a trend–cycle BVAR, Maffei-Faccioli (2025) study the long-run drivers of U.S. GDP growth using sign restrictions on trend components, and conclude that the decline in long-run growth is mainly driven by permanent demand shocks. Ascari and Fosso (2024) analyze the historical drivers of U.S. trend inflation and present evidence consistent with the "globalization of inflation" hypothesis. While they employ a standard trend-cycle BVAR structure, key differences arise in the identification of shocks. Their identification scheme differs between the trend and cycle components, making it challenging to reconcile the structural shocks affecting each component. In contrast, the framework employed in this paper maintains a consistent identification scheme across both trend and cycle components, allowing for a unified interpretation of structural shocks.

The remainder of this paper is structured as follows. In the next section, I introduce the data, detailing its sources and the transformations applied. Section 3 describes the econometric methodology and the shock identification framework. Section 4 presents the empirical decompositions of inflation and real GDP, with Section 4.B focusing on the structural dynamics of trend inflation and the inflation gap, and Section 4.C examining the structural dynamics of potential GDP and the output gap. Finally, Section 5 concludes the paper.

2. Data: Sources, Transformation and Description

Sources. Data are gathered from two main institutions EuroStat and OECD, and back-dated using the Area Wide Model (AWM) database of Fagan, Henry and Mestre (2005). The frequency of the data are quarterly and spans the period 1970Q1-2024Q1. My dataset consists of two blocks, euro area and whole world. From EuroStat's database, I collect for the euro area the following variables: real GDP, unemployment, consumer confidence indicator, Harmonised Index of Consumer Prices (HICP), price perception of households over the next 12 months, unit labor cost index, and energy price index.[9] From OECD's database, I collect the following variables: OCDE's real GDP and HICP - as proxy of the whole world.[10] Finally, my database is characterized by a 'ragged edge', i.e., it has missing values.

Transformations. The series that are not already available in seasonal adjusted form are seasonally adjusted using JDemetra+ 2.2 - this software uses the following algorithm X-13ARIMA-SEATS. Table 1 reports for each variable the name (column 1), mnemonic (column 2), transformation (column 3), and the data span including the back-dated period. A brief comment is needed for variables y^8 and y^9, that represent the GDP and HICP of the world, respectively. These two variables are defined as the ratio between the analogous euro area variable and OECD, representing the euro area's share of world GDP or inflation. This transformation

[9]The consumer confidence and price perception of households over the next 12 months indicators are qualitative surveys, that are reported as aggregated diffusion time series for the euro area. The frequency of these diffusion series is monthly, so I transform them taking quarterly averages.

[10]The identification of distinct global shocks using a limited set of global variables is justified when combined with a robust identification strategy. In this analysis, I adopt the methodological approach proposed by Corsetti et al. (2014) and Bobeica and Jarociński (2019), wherein global and domestic shocks are differentiated through sign restrictions rather than relying on extensive panel datasets.

becomes relevant, in Section 3, to implement the sign restrictions identification proposed by Corsetti, Dedola and Leduc (2014).

Variable name	Symbol	Transformation	Data span
Real GDP	y^1	log	1970.Q1 - 2024Q1
Unemployment Rate	y^2	Δ Q-Q	1970.Q1 - 2024Q1
Consumer Confidence	y^3	none	1985.Q1 - 2024Q1
HICP	y^4	Δlog Q-Q	1970.Q1 - 2024Q1
Price Perception HH	y^5	none	1985.Q1 - 2024Q1
Unit Labor Cost Index	y^6	Δlog Q-Q	1970.Q1 - 2023Q4
Energy Price Index	y^7	log	1987.Q4 - 2024Q1
World Real GDP (WRG)	y^8	log(RGDP^{EA}) - log(WRG)	1970.Q1 - 2024Q1
World HICP (WH)	y^9	Δ (log(HICP^{EA}) - log(WH))Q-Q	1970.Q1 - 2024Q1

Table 1. Description of the variables

3. Econometric Methodology

The model described in this section is the Vector Autoregressive (VAR) model with common trends of Del Negro, Giannone, Giannoni and Tambalotti (2017, 2019), incorporating stochastic volatility (in a similar spirit as Primiceri (2005)) and Student's t-distribution (as in Geweke (1993)).[11] The model decomposes series into slow-moving trends (e.g., potential GDP, trend inflation) and fast-moving cycles (e.g., output-gap, energy price cycle, inflation-gap). Variance-covariance matrices for both components are time-varying, providing an additional hierarchical layer. The identification scheme separates energy, global, and domestic shocks into permanent and transitory components, facilitating volatility assessments over time. Structural drivers are identified using sign-magnitude restrictions.

3.A. The Model: A VAR with Common Trends featuring Stochastic Volatility

The model is given by the measurement equation

$$y_t = \Lambda \bar{y}_t + \tilde{y}_t, \tag{1}$$

where y_t is an n $\times$ 1 vector of observables, $\bar{y}_t$ is a q $\times$ 1 vector of trends, q $\leq$ n, $\Lambda(\lambda)$ is an n $\times$ q matrix of loadings that is restricted and depends on the vector of free parameters λ, and $\tilde{y}_t$ is an n $\times$ 1 vector of stationary components. The rank of Λ, which is equal to q, determines the number of common trends, and the number of cointegrating relationships is therefore n - q. Hence, $\Lambda(\lambda)$ maps the trend component $\bar{y}_t$ to the dependent variable y_t. Both $\bar{y}_t$ and $\tilde{y}_t$ are latent variables and evolve according to the following transition equations, a random walk with

[11] An extension with time-varying autoregressive coefficients following Primiceri (2005) is explored in ongoing research.

drift

$$\bar{y}_t = \bar{c} + \bar{y}_{t-1} + \epsilon_t, \text{ with } \epsilon_t \sim \mathcal{N}(0, \Sigma_t^{\epsilon}), \tag{2}$$

and a VAR

$$\tilde{y}_t = \sum_{j=1}^{P} A_j \tilde{y}_{t-j} + u_t, \text{ with } u_t \sim \mathcal{N}(0, \Sigma_t^{u}) \tag{3}$$

respectively, where the $A_j s$ are n×n matrices.[12]

In this model, the shocks affecting the trend (ϵ_t) and the cycle (u_t) are orthogonal to one another. This implies that my model is a type of "independent trend/cycle decomposition". See Watson (1986), Stock and Watson (1988), and Stock and Watson (2007),for an introduction in standard unobserved component models. This assumption helps introducing in a standard way, time-varying elements in the covariance matrices of the trend and cycle, and a common identification scheme of the structural shocks for the trend and cycle.

The covariance matrices of the error terms ϵ_t and u_t - Σ_t^{ϵ} and Σ_t^{u} - have time-varying elements. The modelization and its core assumptions follow Primiceri (2005), Benati and Mumtaz (2007) and Galí and Gambetti (2009). The structure of the heteroscedastic unobservable shocks is very similar for the permanent and stationary shocks, with two main differences: 1. The dimension of Σ_t^{ϵ} is a q×q matrix, and Σ_t^{u} is of dimension n×n. 2. The innovations of the cycle feature fat-tails and stochastic volatility, while the innovations of the trend only include stochastic volatility. The stochastic volatility helps to capture standard-frequency movements at the cycle's and trend's volatility, see Stock and Watson (2007) for a univariate representation. While, the fat-tails elements capture outliers and extreme realizations over time in the cycle, for example the COVID lockdown.

I consider the following structure for the covariance matrices,

$$\Sigma_t^{\epsilon} = \Phi_{\epsilon,t}^{-1} H_{\epsilon,t} (\Phi_{\epsilon,t}^{-1})', \tag{4}$$

$$\Sigma_t^{u} = \Phi_{u,t}^{-1} H_{u,t} (\Phi_{u,t}^{-1})', \tag{5}$$

where $\Phi_{\epsilon,t}$ and $\Phi_{u,t}$ are lower triangular matrices with elements $\phi_{ij,t}^{\epsilon}$ and $\phi_{ij,t}^{u}$, respectively. $H_{\epsilon,t}$ is a diagonal matrix with diagonal elements $h_{i,t}^{\epsilon}$, while $H_{u,t}$ is a diagonal matrix with diagonal elements $h_{i,t}^{u}$ and $\delta_{i,t}$ - $diag\left(\frac{h_{1,t}^{u}}{\delta_{1,t}}, \cdots, \frac{h_{i,t}^{u}}{\delta_{i,t}}, \cdots, \frac{h_{n,t}^{u}}{\delta_{n,t}}\right)$.

The structure of Φ_t^z, where z = { ϵ, u}, is

$$\Phi_{z,t} = \begin{pmatrix} 1 & 0 & \dots & 0 \\ \phi_{21,t}^{z} & 1 & \ddots & \vdots \\ \vdots & \ddots & \ddots & 0 \\ \phi_{k1,t}^{z} & \dots & \phi_{kk-1,t}^{z} & 1 \end{pmatrix},$$

[12]The drift is incorporated in the trend of variables that enter in levels and contain a time-trend, such as euro area GDP, energy price index, and the ratio between the euro area and world GDP.

where the elements in each row follow

$$\phi^z_{i,t} = \phi^z_{i,t-1} + V^z_{i,t}, \text{Var}\left(V^z_{i,t}\right) = D^z_i, \tag{6}$$

for $i = 1 \cdots k$, where k = { q, n}. I assume that the non-zero and non-one elements of $\Phi_{z,t}$ belonging to different rows evolve independently, with

$$D^z = \begin{bmatrix} D^z_1 & 0_{1\times 2} & \dots & 0_{1\times(k-1)} & 0_{1\times k} \\ 0_{2\times 1} & D^z_2 & \ddots & 0_{2\times k-1} & 0_{2\times k} \\ \vdots & \ddots & \ddots & \ddots & \vdots \\ 0_{(k-1)\times 1} & 0_{k-1\times 2} & \ddots & D^z_{k-1} & 0_{(k-1)\times k} \\ 0_{k\times 1} & 0_{k\times 2} & \ddots & 0_{k\times(k-1)} & D^z_k \end{bmatrix}.$$

In other words, $V^z_{i,t}$ and $V^z_{j,t}$ are uncorrelated for j ≠ i.

The structure of H^ϵ_t and H^u_t is

$$H_{\epsilon,t} = \begin{bmatrix} h^\epsilon_{1,t} & 0 & \dots & 0 \\ 0 & h^\epsilon_{2,t} & \ddots & \vdots \\ \vdots & \ddots & \ddots & 0 \\ 0 & \dots & 0 & h^\epsilon_{q,t} \end{bmatrix}, H_{u,t} = \begin{bmatrix} \frac{h^u_{1,t}}{\delta_{1,t}} & 0 & \dots & 0 \\ 0 & \frac{h^u_{2,t}}{\delta_{2,t}} & \ddots & \vdots \\ \vdots & \ddots & \ddots & 0 \\ 0 & \dots & 0 & \frac{h^u_{n,t}}{\delta_{n,t}} \end{bmatrix},$$

with

$$\ln h^\epsilon_{i,t} = \ln h^\epsilon_{i,t-1} + Z^\epsilon_{i,t}, \text{Var}\left(Z^\epsilon_{i,t}\right) = g^\epsilon_i, \tag{7}$$

$$\ln h^u_{i,t} = \ln h^u_{i,t-1} + Z^u_{i,t}, \text{Var}\left(Z^u_{i,t}\right) = g^u_i, \tag{8}$$

, with slithery abuse of notation, for $i = 1 \cdots$ q / n. I assume that $Z^z_{i,t}$ and $Z^z_{j,t}$ are uncorrelated for j ≠ i, with

$$G^z = \begin{bmatrix} g^z_1 & 0 & 0 & 0 \\ 0 & g^z_2 & 0 & 0 \\ 0 & 0 & \ddots & 0 \\ 0 & 0 & 0 & g^z_k \end{bmatrix}.$$

In line with Geweke (1993), the weights $[\delta_{1,t}, \delta_{2,t}, \cdots, \delta_{n,t}]$ are indexed by time t, since they are meant to capture extreme volatility movements (fat-tails) over time in the cycle, hence potentially providing an effective treatment of outliers and extreme events. $[h^1_{n,t}, h^2_{n,t}, \cdots, h^u_{n,t}]$ captures standard-frequency movements in the cycle's volatility. It is worth noting the following

relationships

$$\Phi_{\epsilon,t}(H_{\epsilon,t})^{-1/2}\epsilon_t = w_t^{\epsilon}, \text{Var}\left(w_t^{p}\right) = I_q,$$
$$\Phi_{u,t}(H_{u,t})^{-1/2}u_t = w_t^{u}, \text{Var}\left(w_t^{t}\right) = I_n.$$

Hence, as shown by Geweke (1993), assuming a Gamma prior for $\delta_{i,t}$ of the form $p(\delta_{i,t}) = \prod_{t=1}^{T} p(\delta_{i,t}) = \prod_{t=1}^{T} \tilde{\Gamma}(1, \kappa_{\delta,i})$ leads to a scale mixture of normals for the orthogonal residuals w_t^u, with mean 1 and degrees of freedom $\kappa_{\delta,i}$.[13] This assumption allows the degrees of freedom for the Student's t-distribution to be independent across equations and simplifies the estimation algorithm. To further simplify the estimation of the model, I assume that w_t^{ϵ}, w_t^u, V_t^{ϵ}, V_t^u, Z_t^{ϵ}, Z_t^u are mutually uncorrelated.[14]

As discussed earlier, there are two noteworthy things about this type of trend-cycle model. First, the model decomposes observed variables (y_t) into some slow-moving variables (trends) and fast-moving variables (cycles). Second, this model has two sets of time varying 'coefficients' $\phi_{ij,t}^{\epsilon}$ and $\phi_{ij,t}^{u}$ - for the trend and cycle parts -, two stochastic volatility parameters for the diagonal elements of each component, $h_{i,t}^{\epsilon}$ and $h_{i,t}^{u}$, and fat-tails ($\delta_{i,t}$) that capture infrequent volatility movements over time in the cycle.

Discussion. Using both stochastic volatility (SV) and Student's t-distributions might initially seem redundant, as SV alone already implies a fat-tailed unconditional distribution. However, incorporating Student's t-distributions addresses two specific issues in this application. Firstly, without Student's t-distributions, the degrees of freedom governing the expected volatility changes in trends must be substantially increased. This higher value tightens prior beliefs excessively, creating an almost direct mapping between posterior and prior distributions. Consequently, without Student's t-distributions and at lower degrees of freedom, the volatility and trend components mimic higher-frequency variations, overly suppressing cyclical dynamics. For instance, Del Negro et al. (2017, 2019) use 100 degrees of freedom on diagonal elements of trend covariance matrices in a model with time-invariant covariance matrices.[15]

Secondly, the posterior distributions of the degrees of freedom across the cyclical components suggest that the inclusion of Student's t-errors is empirically justified. As shown in Figure 25, most variables exhibit posterior densities concentrated in the range of 5 to 20 degrees of freedom.

[13] This formulation is equivalent to a specification that assumes Student's t-distribution for w_t^u with $\kappa_{\delta,i}$ degrees of freedom.

[14] These assumptions advocate for a block-diagonal structure for the joint set of innovations in the model. This is convenient for several reasons: First, parsimony, as the model is already quite heavily parameterized. Second, as discussed earlier, it heavily simplifies the estimation algorithm. Third, similar structures are used in other types of model, e.g. TVP-VAR-SV models - see Primiceri (2005, pp. 6-7).

[15] In the context of this application, the prior distribution in Del Negro et al. (2017, 2019) corresponds to an equivalent prior specification with 50 degrees of freedom. The prior distribution in Del Negro et al. (2017, 2019) follows an Inverse-Wishart specification. The Inverse-Wishart distribution is the multivariate generalization of the inverse gamma distribution. Consequently, for a 1×1 variance parameter, the Inverse-Wishart reduces to an inverse gamma distribution. Specifically, if Σ represents a scalar variance σ^2, then $\Sigma \sim$ Inverse-Wishart(ν, Ψ) simplifies to $\sigma^2 \sim$ Inverse-Gamma(α, β), where $\alpha = \frac{\nu}{2}$ and $\beta = \frac{\Psi}{2}$. Thus, an $n \times n$ Inverse-Wishart prior with $\nu = 100$ implies that each variance term follows an inverse gamma distribution with a prior strength equivalent to $\alpha = 50$.

This range is typically associated with moderately fat-tailed behavior. For some cycles, such as the ones related to consumer confidence, household price perception, or energy prices, the posterior mode lies even closer to the lower end of this spectrum (DOF $\approx$ 3–6), highlighting the presence of heavy-tailed shocks that stochastic volatility alone cannot capture. These findings align with the macroeconomic literature, which shows that Student's t-distributions improve the fit and density forecasting performance of macroeconomic models, particularly when combined with stochastic volatility (e.g., Cúrdia et al., 2014; Clark and Ravazzolo, 2015; Chiu et al., 2017).

Finally, in this study, the assumption of independence is adopted intentionally because it clearly delineates permanent from cyclical components, simplifies structural shock identification and facilitates the estimation of the time-varying covariance matrices, and ensures interpretative transparency by aligning long-run forecasts with the trend component.[16] Nevertheless, in ongoing research I further explore the possibility of relaxing this assumption by integrating dependency and time variation.[17]

Baseline specification. In the baseline specification, y_t contains nine macroeconomic variables, see table 2. Column two and three describe the macroeconomic trends (five in total - q = 5), and cycles (nine in total - n = 9) characterizing the set of variables in the system. The estimation sample spans the period 1990Q1-2024Q1.[18]

Variable name	Trend	Cycle
Real GDP	Potential GDP	Output Gap
Δ Unemployment Rate	none	Unemployment Cycle
Consumer Confidence	none	Consumer Confidence Cycle
HICP	Trend Inflation	Inflation Gap
Price Trends next 12 m	Trend Inflation	Price Expectation Cycle
Unit Labor Cost Index	Trend Inflation	Labor Cost Cycle
Energy Price Index	Trend Energy	Energy Price Cycle
World GDP	Potential WGDP	World Output Gap
World HICP	Trend W Inflation	World Inflation Gap

Table 2. Description of the variables

Slow-moving variables: 1. The EA output trend - that I label as EA potential GDP - is restricted to be common across only real EA GDP.[19]

[16]The consideration of standard correlated trends and cycles, as in Beveridge-Nelson decompositions, often results in excessively volatile trends, diminishing the cyclical fluctuations - large in amplitude, persistent, and procyclical- typically emphasized by policymakers.

[17]To address excessively volatile trends, previous research has recommended imposing a low signal-to-noise ratio in the underlying autoregressive model, as shown by Kamber et al. (2018), Morley et al. (2024), Kamber et al. (2025), Morley and Wong (2020), or González-Astudillo and Roberts (2022).

[18]The series used in the baseline specification are available, some of them, from 1970Q1 - see table 1. The period 1970Q1-1989Q4 is used as presample to inform the priors on the initial conditions of the trend and the cycle, which I discuss in the next section.

[19]The drift coefficient in the unit root process, that constantly accumulates over time, can be thought as an average effect of technological innovation.

2. The persistent component of inflation (trend inflation) is extracted using the information in inflation, households' perceived inflation, and the unit labor cost (a proxy for firms' inflation expectations).[20] Unit labor costs (defined as the growth of nominal wage adjusted per employee) play a role in shaping firms' inflation expectations by influencing future firms' pricing decisions. In theoretical models, the unit labor cost and price inflation are closely interrelated in the medium / long-run. This is due to prices and nominal wages must adjust relative to each other to be consistent with the fact that, in the long-run, the real wage is determined by slow-moving factors such as productivity, wage demands or bargaining power.[21] As shown in C Table 5, the Johansen cointegration rank test rejects the null hypothesis of no cointegration $r = 0$ and also rejects $r \leq 1$ when tested against the alternative $r \geq 2$, but fails to reject $r \leq 2$ against $r = 3$. These results indicate the presence of one common trend among the three variables. Figure 10 (Appendix C) plots the prior and posterior distributions of the cointegrating coefficients that link inflation, household inflation expectations, and unit labor costs. The posterior distributions deviate noticeably from the priors, suggesting that the data are informative about the common component among these variables and support the existence of a stable cointegrating vector.[22]

3. The energy trend which is restricted to be common to EA energy prices. This assumption is standard to be able to estimate an 'energy price cycle', see Hasenzagl et al. (2018). Moreover, Kilian (2008) highlights the important influence of energy prices on economic performance. In particular, Kilian points to the role of energy price fluctuations. In principle, permanent disturbances coming from energy prices should be very low, since the major movements in energy prices should come from the cycle part (which have a temporary influence on the economy).

4. The fourth and fifth trends denote the world potential output and world trend inflation. These two trends are of core use if one seeks to understand the importance of global supply and demand shocks. In particular, to address whether global demand–supply imbalances have potential permanent effects.

The main reason for estimating five trends is to identify the following permanent shocks: domestic demand and supply-side factors, energy supply factors, and global demand and supply-side factors. The identification scheme is presented in the next section.

[20] Recently, Candia, Coibion and Gorodnichenko (2021) show that firms' inflation expectations exhibit many of the characteristics of households' inflation expectations and dramatically depart from the inflation expectations of professional forecasters. Moreover, recent empirical evidence for the euro area (e.g. Álvarez and Correa-López (2020)) shows that time series that contain information about households' and firms' perceived inflation are better at predicting inflation than professional forecasters or financial markets - in the context of open economy Phillips curves. In another work, Coibion and Gorodnichenko (2015) present new econometric and survey evidence consistent with firms having similar expectations as households. Moreover, they show evidence that inflation expectation of professional forecasters do not proxy well the expectations of households.

[21] In my model, labor cost inflation and price inflation are cointegrated. Then, gradual changes in the long-run labor cost inflation are mapped to the trend inflation. This assumption implies that in the cost of living enter the dynamics of nominal wages. Hence, I am capturing potential second-round reactions of the labor cost to actual inflation.

[22] For the case of the euro area, in a recent paper of Bobeica et al. (2019), they, find that there is a clear link between the rate of change in labor cost and the rate of change in prices. Moreover, they find that this link becomes stronger when inflation is high. However, in this paper I do not explore that this link could depend on an inflation regime, given that it would make the second part of structural analysis too difficult and cumbersome.

Fast-moving variables: The macroeconomic cycles are characterized by the same number of variables in the system, nine. This implies that each variable in the system has its own idiosyncratic cycle component. Notice that the consumer confidence indicator and differences in the unemployment rate are left trendless.[23] Finally, the information gathered within the interrelation of these macroeconomic cycles - output gap ($\tilde{y}^1$), unemployment cycle ($\tilde{y}^2$), consumer confidence ($\tilde{y}^3$), inflation gap ($\tilde{y}^4$), price expectation cycle ($\tilde{y}^5$), labor cost cycle ($\tilde{y}^6$), energy price cycle ($\tilde{y}^7$), world output gap ($\tilde{y}^8$), and world inflation cycle ($\tilde{y}^9$) - can be compared to a Dynamic Stochastic General Equilibrium (DSGE) model. To be more precise, the cycle VAR structure nests several structural models, for example: (i) a range of Phillips curve models, since inflation can be a purely forward-looking process, driven by expectations on inflation (price expectation cycle) or expectations of future real economic activity (consumer confidence). Moreover, it integrates 'the triangle model of inflation', where potential fluctuations of inflation in response to the temporary influence of movements in energy prices (energy price cycle), the degree of resource utilization in the economy (output-gap and unemployment cycle).[24] To understand inflation dynamics from an open economy perspective, it also takes into account a global Phillips curve part.[25] (ii) From the perspective of the EA output-gap, it features the inverse relation of the Okun's law since output is linked to unemployment fluctuations. Moreover, it captures how slack in real output is affected when potential international political events arise – as is the case for oil price, food and beverages, and the recent global supply bottlenecks. Hence, my model accounts for a wide variety of sources that can modify the interrelation of these macroeconomic cycles.

3.B. Priors and Estimation Procedure

Priors. First, I need to specify a distribution for the initial conditions $\bar{y}_0$ and $\tilde{y}_{0:-p+1} = (\tilde{y}_0', \cdots, \tilde{y}_{-p+1}')'$ are distributed according to $\bar{y}_0 \sim \mathcal{N}\left(\underline{y_0}, I_q\right)$ and $\tilde{y}_{0:-p+1} \sim \mathcal{N}\left(0, \underline{\Sigma_0^{\mathcal{A}}}\right)$, where $\underline{y_0}$ and $\underline{\Sigma_0^{\mathcal{A}}}$ are computed using pre-sample data.

Starting with the prior for $\Lambda(\lambda)$ is given by $p(\lambda) = N(1, 0.5^2)$, the product of independent

[23] The consumer confidence indicator is included in its original, untransformed form, as by definition is intended to capture short-term developments in economic activity. The unemployment rate, on the other hand, is incorporated in quarterly differences due to the presence of a unit root, as shown in Appendix C, Table 6. It is worth noting that if the unemployment rate were included in levels, it would be possible to estimate a new trend component, thereby allowing for the identification of a new structural shock related to the trend, such as labor supply shocks. However, the primary objective of this paper is to identify core structural shocks rather than their subcomponents, particularly in the context of domestic supply shocks. For a detailed discussion of identifying structural shocks on the supply side—including technology, labor supply, wage bargaining, and matching efficiency—see Foroni et al. (2018). Furthermore, the inclusion of Δ unemployment and the consumer confidence indicator is important for the accurate estimation of the stationary component of GDP, the output gap. Indeed, these two variables are central to core now-casting models, which are widely employed by many central banks. See Laxton and Tetlow (1992), Kamber et al. (2018), and Barbarino et al. (2020) for a more contemporary perspective.

[24] See Gordon (1981, 1988). Moreover, it reflects the view of Yellen (2016) which is widely shared by policy makers and central bankers. See also the work of Hasenzagl et al. (2018) that emphasizes the inclusion of an energy price cycle.

[25] The importance of including cyclical global activity measures is suggested in Martínez-García and Wynne (2010); Kabukçuoğlu and Martínez-García (2018); Duncan and Martínez-García (2023).

Gaussian distributions for each element λ of the matrix $\Lambda(\lambda)$. The drift $\bar{c}$ incorporated in the random walks of the trends is assumed to follow a diffuse normal prior, $\mathcal{N}(\underline{c}_{y,0}, 10)$ with mean $\underline{c}_{y0}$, that represents the average growth rate of the pre-sample variables. The priors for the VAR coefficients $\mathcal{A} = (A_1, \ldots, A_p)$ have a normal posterior distribution with mean $\bar{\mathcal{A}}$ and variance $\bar{\Sigma}^{\mathcal{A}}$, based on prior mean $\underline{\mathcal{A}}$ and $\underline{\Sigma}_0^{\mathcal{A}}$, where:

$$(\bar{\Sigma}^{\mathcal{A}})^{-1} = (\underline{\Sigma}_0^{\mathcal{A}})^{-1} + \sum_{t=1}^{T} \left((\Sigma_t^u)^{-1} \otimes \tilde{x}_t \tilde{x}_t' \right),$$

$$\text{vec}(\bar{\mathcal{A}}) = \bar{\Sigma}^{\mathcal{A}} \left\{ \text{vec} \left(\sum_{t=1}^{T} (\Sigma_t^u)^{-1} \tilde{y}_t \tilde{x}_t' \right) + (\underline{\Sigma}_0^{\mathcal{A}})^{-1} \text{vec}(\underline{\mathcal{A}}) \right\} I(\text{vec}(\underline{\mathcal{A}})),$$

$\tilde{x}_t$ contains the lags of $\tilde{y}_t$ and $I(\text{vec}(\underline{\mathcal{A}})$ is an indicator function that is equal to 0 if the VAR is explosive - some of the eigenvalues of $\mathcal{A}(L)$ are greater than 1 - and to 1 otherwise. Hence, I am enforcing a stationarity constraint on the VAR. Moreover, the prior for the VAR parameters $\text{vec}(\underline{\mathcal{A}})$, describing the components $\tilde{y}_t$, is a standard Minnesota prior with the hyperparameter for the overall tightness equal to the commonly used value of 0.2 (see Giannone, Lenza and Primiceri (2015)), and centered at zero rather than one, since I am dealing with stationary processes. Finally, the VAR uses four lags (p = 4).

The priors for the variance-covariance time-varying elements follows Benati and Mumtaz (2007) and Geweke (1993), with some minor modifications to take into account the important differences between the permanent (Σ_t^{ϵ}) and transitory (Σ_t^u) matrices governing each process. Prior distributions for the time-varying elements in the permanent side are going to be scaled down by a factor of one hundred. Such a choice is clearly arbitrary, but motivated by my goal of informing to the model that the former elements should have much lower volatility than its counter part (the transitory elements). In other words, the elements belonging to the slow-moving variables should resemble two features: (i) low volatility in magnitude and (ii) low expected changed in volatility. This approach helps me to deal with the problem of label switching in mixture models in order to reliably recover the entire posterior distribution.[26]

Following Geweke (1993), I set a hierarchical Gamma prior on the parameter controlling the degree of freedom of the Student's t distributions $\kappa_{\delta,i}$ and the weighting vector $\delta_{i,t}$, for $i = 1, \ldots, n$:

$$p(\kappa_{\delta,i}) \sim \tilde{\Gamma}(n_0, 2),$$
$$p(\delta_{i,t}) \sim \tilde{\Gamma}(1, \kappa_{\delta,i}).$$

The prior mean n_0 is assumed to equal 20. This allocates a substantial prior weight to fat-tailed distributions as well as distributions that are approximately Normal. In order to calibrate the prior distributions for $\phi_{ij,0}^z$ and $h_{i,0}^z$, I 'estimate' a time-invariant version of 1 based on an unbalanced dataset, from 1970 Q1 to 1989 Q4.[27] Let Σ_0^z be the estimated variance-covaraince

[26] See Geweke (2007) and Stephens (2000).

[27] This is not a real estimation. I run just a few iterations MCMC to decompose the pre-sample data into

matrices from the time-invariant decomposition model. Let L^z be the lower-triangular Choleski factor of Σ_0^z - i.e., $L^z L^{z'} = \Sigma_0^z$. The initial conditions for the stochastic volatily process, $\ln h_0^u$ and $\ln h_0^\epsilon$, are set to follow a $\mathcal{N}(\ln \mu_0^u, 10 \times I_n)$ and $\mathcal{N}(\ln \mu_0^\epsilon, 0.1 \times I_q)$, respectively. The prior means, $\mu_0^z = \{\mu_0^\epsilon, \mu_0^u\}$ is a vector collecting the logarithms of the squared elements on the diagonal of L^z. Then each column of L^z is divided by the corresponding element on its diagonal - i.e., $\tilde{L}^z$ are the rescaled matrices - and set the initial conditions of the elements below the diagonal, $\phi_{ij,0}^u$ and $\phi_{ij,0}^\epsilon$, to follow a $\mathcal{N}(\tilde{\phi}_{ij,0}^u, \tilde{V}(\tilde{\phi}_{ij,0}^u))$ and $\mathcal{N}(\tilde{\phi}_{ij,0}^\epsilon, \tilde{V}(\tilde{\phi}_{ij,0}^\epsilon))$, respectively. The prior means of $\tilde{\phi}_{ij,0}^z$ are the non-zero and non-one elements of $(\tilde{L}^z)^{-1}$ (i.e., the elements below the diagonal). The variance-covariance matrices, $\tilde{V}(\tilde{\phi}_{ij,0}^u)$, are postulated to be diagonal with each individual (i,i) element equal to the absolute value of the corresponding $\tilde{\phi}_{ij,0}^z$.

The matrices in D^z are also calibrated following Benati and Mumtaz (2007). D^z follow a diffuse inverse Wishart - $p\left(D_i^z\right) = IW\left(\kappa_{D,i}, \kappa_{D,i}(\eta_z \underline{D_i^z})\right)$ - with just enough prior degrees of freedom, $\kappa_{D,i}$, set equal to the number of rows in $\underline{D_i^z}$ plus two to have a well-defined prior mode. The mode $\underline{D_i^z}$ is scaled by the number of degrees of freedom and $\eta_{u,\epsilon} = \{10^{-3}, 10^{-5}\}$. Each $\underline{D_i^z}$ is composed of the row elements below the diagonal in $\tilde{L}^z$.

Finally, as for the variances of the stochastic volatility innovations (i.e., the diagonal elements of G^z), I follow Cogley and Sargent (2005). They postulate an inverse-Gamma distribution, $g_j^z \sim IG\left(\frac{\kappa_G}{2}, \frac{\underline{g_i^z}}{2}\right)$, for the elements of G^z with κ_G degrees of freedom and prior mode $\underline{g_i^z}$. I use different prior modes to take into account the important differences between the permanent (G^u) and transitory (G^ϵ) volatility innovations. In this way, I am informing the model to not mix permanent and transitory volatility processes. For the stochastic volatility innovations from the transitory part, I use the same specifications as Cogley and Sargent (2005), $g_j^u \sim IG\left(\frac{1}{2}, \frac{10^{-4}}{2}\right)$. The choice of for the stochastic volatility innovations belonging to the permanent part are chosen accordingly to represent specific features. In this sense, I set the mode of diagonal elements of the matrix $\underline{G^\epsilon} = \{\underline{g_1^\epsilon}, \underline{g_2^\epsilon}, \underline{g_3^\epsilon}, \underline{g_4^\epsilon}, \underline{g_5^\epsilon}\}$ to $\underline{G^\epsilon} = \{8.3 * 10^-6, 3.3 * 10^-5, 8.6 * 10^-5, 8.3 * 10^-6, 3.3 * 10^-5\}$. A priori, it implies that the expected change over a period of a hundred years in the volatility of potential GDP, inflation trend, energy trend, potential world GDP, and world inflation trend is 0.33, 1.33, 3.33, 0.33, 1.33 percentage points, respectively.[28] In addition, these priors are weakly more informative than the previous ones, with the degrees of freedom set to five (i.e., $\kappa_G = 5$).[29] There are two intrinsic reasons for the selection of these priors: (i) to ensure these do not reflect business cycle fluctuations; and (ii) to a priori prevent scenarios such as de-anchoring of long-term inflation trend. Nevertheless, if data spoke loudly in favor of relevant movements in the low-frequency components of the system, it would push away from the prior assumptions.[30]

trends and cycles, and obtain the matrices of interest. Notice that this procedure yields 'naive' elements (i.e., $\phi_{ij,0}^\epsilon, \phi_{ij,0}^u, h_{i,0}^\epsilon$ and $h_{i,0}^u$).

[28] Relative to the ones of the cycle component, the current prior mean values exhibit reductions by factors of 12 for GDP trends, 3 for inflation trends, and 1.2 for energy trends.

[29] However, this specification remains considerably less restrictive than those used in standard trend-cycle models, where the degrees of freedom are typically set to 100 (e.g., Del Negro et al. (2017, 2019)).

[30] While in the baseline specification I specify the same prior on the variance-covariance matrix of the trend components for the euro area and the world, this could be in principle different for the two region components.

Estimation. The state-space model, given by equations 1 through 8, is efficiently estimated with Bayesian methods - Gibbs Sampling and Metropolis Hastings algorithm - using Kalman Filter, in conjunction with modern simulation smoothing techniques (Carter and Kohn (1994)) that easily help me to accommodate missing observations, and draw the latent states. All results are based on 150,000 simulations, of which I discard the first 142,000 as burn-in draws and save every 15th draw in order to reduce the autocorrelation across draws.[31] Section A of the appendix describes the Gibbs sampler, which accommodates the hierarchical decomposition model to different modeling choices.

3.C. Shock Identification Strategy

As discussed in the introduction, this study identifies the shocks most emphasized in the inflation literature. These structural factors include energy supply, global and domestic shocks, from a demand and supply view. Each of these is analyzed from both a permanent and transitory perspective to gain a comprehensive understanding of inflation dynamics.

To derive economically meaningful conclusions regarding the transmission channels of these shocks, restrictions must be imposed on the variance-covariance matrices $(\Sigma_t^{\epsilon}, \Sigma_t^{u})$. These restrictions enable the mapping of economically interpretable structural shocks from the estimated reduced-form residuals. In this framework, the relationship between reduced-form and structural trend residuals is defined as $\epsilon_t = B_t w_t^P$, where B_t is a non-singular matrix satisfying $B_t B_t' = \Sigma_t^{\epsilon}$. The structural permanent shocks, denoted as w_t^P, follow a standard normal distribution $w_t^P \sim N(0_{q,1}, I_{q,q})$ with unit variance. Similarly, the mapping between reduced-form and transitory structural residuals is given by $u_t = C_t w_t^T$, where C_t is a non-singular matrix satisfying $C_t C_t' = \Sigma_t^{u}$. The structural transitory shocks, represented by w_t^T, also follow a standard normal distribution $w_t^T \sim N(0_{n,1}, I_{n,n})$ with unit variance.

The latent variables—i.e., trends and cycles—introduced in equation 1 can be rewritten as follows:

$$
\begin{aligned}
y_t =& \Lambda\Big(\bar{y}_0 + \sum_{h=1}^{t} h\bar{c} + \sum_{j=0}^{t-1} \epsilon_{t-j}\Big) + \sum_{j=0}^{t-1} \tilde{A}_j u_{t-j} \\
=& \Lambda\Big(\bar{y}_0 + \sum_{h=1}^{t} h\bar{c} + \sum_{j=0}^{t-1} B_{t-j} B_{t-j}^{-1} \epsilon_{t-j}\Big) + \sum_{j=0}^{t-1} \tilde{A}_j C_{t-j} C_{t-j}^{-1} u_{t-j} \\
=& \Lambda\Big(\bar{y}_0 + \sum_{h=1}^{t} h\bar{c}\Big) + \Lambda \underbrace{\sum_{j=0}^{t-1} B_{t-j} w_{t-j}^P}_{\text{Contribution of Permanent Shocks}} + \underbrace{\sum_{j=0}^{t-1} \tilde{A}_j C_{t-j} w_{t-j}^T}_{\text{Contribution of Transitory Shocks}} .
\end{aligned}
\tag{9}
$$

This formulation is derived by applying successive substitution for $\bar{y}_{t-j}$ and $\tilde{y}_{t-j}$, where $\tilde{A}_j$

[31] I assess the convergence of the Markov chain by inspecting the autocorrelation properties of the ergodic distribution's draws. Moreover, I follow the diagnostic for monitoring the convergence of multiple Metropolis Hastings chains of Geweke et al. (1991). The inefficiency factors for all posterior elements are represented in Figure 9 of Appendix B.

represents the companion form matrix raised to the power of horizon j. It further incorporates the mapping between reduced-form and structural residuals. Here, B_t is interpreted as $\mathrm{d}\bar{y}_t/\mathrm{d}w_t^P$, while $\tilde{A}_j C_{t+j}$ represents $\mathrm{d}\tilde{y}_{t+j}/\mathrm{d}w_t^T$. These terms quantify the effects of shocks on the low- and high-frequency components, respectively. In fact, equation 9 provides the full historical decomposition of each variable in terms of permanent and transitory structural shocks, reflecting deviations from initial conditions and the drift of the respective trend.

The structural identification in this study relies on sign and magnitude restrictions. First, I follow Canova and De Nicolo (2002) in order to distinguish between demand-side and supply-side factors. This identification strategy is based on the premise that supply-side forces drive output and inflation in opposite directions, whereas demand-side forces result in a positive comovement. Second, to differentiate between domestic and global shocks, the approach builds on the comovements proposed by Corsetti et al. (2014), which state that global shocks have a greater impact on global variables than on domestic ones, and vice versa for domestic shocks.[32] To effectively implement this restriction, world GDP and inflation must be expressed as the ratio of euro area to world values, as outlined in Section 2.

For example, if a shock leads to an increase in real EA GDP while simultaneously raising the EA's share of global GDP, it can be inferred that the shock had a stronger impact on the domestic economy relative to the rest of the world, classifying it as a domestic shock. Conversely, if the shock decreases the euro area's share of global GDP, it suggests a greater impact on the rest of the world, categorizing it as a global shock. A global supply shock, for instance, would raise both euro area and world GDP, but more strongly abroad $(+/(++))$, thereby reducing the euro area's share of global GDP. Likewise, on the inflation side, this same shock would lower both euro area and world inflation, with a larger decline in world inflation $(-/(--))$; this implies an increase in the euro area's share of global inflation (i.e., the share rises because the world component falls more than the euro-area component). A positive energy supply shock would lower energy prices, positively impact euro area real activity, and reduce euro area inflation upon impact. These restrictions align with findings in the literature on energy-related shocks, such as Kilian (2009), who models the global crude oil market and examines the effects of such shocks on key macroeconomic variables.[33] Additionally, it is assumed that energy supply shocks have a greater impact on the euro area due to its high energy dependence relative to the rest of the world.[34]

A domestic supply shock is expected to have a smaller absolute effect on energy prices compared to an energy supply shock, represented as $|e_{ds}| < |e_{es}|$, where e_{ds} and e_{es} denote the responses of energy prices to domestic supply and energy supply shocks, respectively. In other words, a contraction in energy supply capacity leads to a greater increase in energy prices than a

[32] Other empirical studies employing similar methodologies to distinguish between global and domestic shocks include Bobeica and Jarociński (2019) and Conti et al. (2017).

[33] Peersman and Van Robays (2009) analyze the commovements of energy prices and euro area economic activity following an energy supply shock. Such a shock increases energy prices and has negative real activity effects.

[34] Currently, the euro area has an energy import dependency rate of approximately 60%.

reduction in domestic economic activity. Similarly, an expansion in energy supply capacity has a stronger downward effect on energy prices than a comparable expansion in domestic economic activity, such that $e_{ds} > e_{es}$.

The identification algorithm is based on the sign restrictions methodology developed by Canova and De Nicolo (2002) and Uhlig (2005), with refinements by Rubio-Ramirez, Waggoner and Zha (2010) and Arias, Rubio-Ramírez and Waggoner (2018).[35] This approach employs the Haar prior, which, as discussed in Baumeister and Hamilton (2015), results in non-uniform marginal priors for individual impulse responses.[36] However, Arias, Rubio-Ramirez and Waggoner (2023) argue that this property is inconsequential for joint inference, demonstrating that the Haar prior ensures a uniform joint prior distribution over the identified set of impulse responses, meaning no specific structural vector is favored a priori. In fact, Arias et al. (2023) show that with a sufficiently tight identification the influence of the prior diminishes, allowing the data to drive posterior inference, consistent with the findings of Inoue and Kilian (2022). This identification strategy is implemented similarly to traditional SVARs with sign restrictions. The key distinction is that while structural VAR analysis typically focuses on business cycle fluctuations, this study also aims to identify factors influencing low-frequency movements.

The sign–magnitude restrictions identify five economically meaningful shock domains spanning both the trend and cyclical components: domestic supply, domestic demand, global supply, global demand, and energy supply. At the cyclical frequency, however, the restrictions do not uniquely pin down all individual shocks within these domains. In particular, the cyclical block is identified only up to four orthogonal rotations. If left unrestricted, these residual rotations can mix innovations across the economically meaningful shock domains already labeled by the sign–magnitude restrictions—a version of the "masquerading problem" emphasized by Wolf (2020, 2022). To ensure that the reported results do not depend on an arbitrary within-domain rotation, I proceed in two steps. First, I recover an admissible set of nine shocks consistent with the sign–magnitude restrictions: two shocks each for domestic supply, domestic demand, global supply, and global demand, plus one energy supply shock. Second, I report domain-level composite shocks by aggregating the pair of shocks within each domain (domestic supply, domestic demand, global supply, global demand), while leaving the energy supply shock as a standalone fifth shock.[37] I do not impose additional restrictions to label the two shocks within each pair, since the objective is to recover aggregate domestic/global supply and demand effects rather than to further decompose them (e.g., technology vs labor-supply, or fiscal vs monetary vs financial innovations).

Tables 3 and 4 present the set of sign restrictions applied to the permanent and transitory shocks, respectively. The restrictions are consistent across both types of shocks.

[35] Additional details on the sign and magnitude restrictions algorithm are provided in Appendix A.2.

[36] In the case of two variables, the prior is concentrated at extreme values, while for models with more than three variables, it is centered around a zero impact response of shocks.

[37] By construction, the five composite shocks–domestic supply, domestic demand, global supply, global demand, and energy supply–are orthogonal.

Discussion. The use of sign and magnitude restrictions to identify structural shocks on the cyclical side is a standard and widely accepted practice in the structural VAR literature, where such restrictions typically apply to deviations from a deterministic trend. However, imposing similar restrictions on the stochastic trend component—particularly to identify permanent demand-side shocks—may be viewed as more controversial.

	Domestic Supply	Domestic Demand	Energy Supply	Global Supply	Global Demand
EA Potential GDP	+	+	+	+	+
EA Inflation Trend	-	+	-	-	+
Energy Price Trend	- ($\|e_{ds}\| < \|e_{es}\|$)	+	- (e_{es})	-	+
EA/W Potential GDP	+	+	+	-	-
EA/W Inflation Trend	-	+	-	+	-

Table 3. Sign restrictions on trends

	Domestic Supply	Domestic Demand	Energy Supply	Global Supply	Global Demand
Output Gap	+	+	+	+	+
Unemployment Cycle	·	·	·	·	·
Consumer Confidence Cycle	·	·	·	·	·
Inflation Gap	-	+	-	-	+
Price Expectation Cycle	·	·	·	·	·
Labor Cost Cycle	·	·	·	·	·
Energy Price Cycle	- ($\|e_{ds}\| < \|e_{es}\|$)	+	- (e_{es})	-	+
EA/World Output Gap	+	+	+	-	-
EA/World Inflation Gap	-	+	-	+	-

Table 4. Sign restrictions on cycles

Nonetheless, recent empirical work has made substantial progress in this area. Studies such as Ascari and Fosso (2024), Furlanetto et al. (2025), and Maffei-Faccioli (2025) provide frameworks to identify both permanent demand and supply shocks. For example, Maffei-Faccioli (2025) investigates the long-run drivers of U.S. GDP growth by applying structural identification to the trend component. Similarly, Ascari and Fosso (2024) identifies the determinants of U.S. trend inflation from both global and domestic sources. While both studies employ comparable empirical settings to disentangle structural shocks along demand-supply and international-domestic dimensions, their identification strategies differ. Ascari and Fosso (2024) imposes sign restrictions on the cointegration relationships between observable variables and trends. In contrast, Maffei-Faccioli (2025) employs sign restrictions directly on the impact matrix (i.e., the variance-covariance structure) of trend innovations—a strategy that mirrors the standard SVAR approach but is applied solely to the trend component.

This paper adopts the identification method of Maffei-Faccioli (2025) due to its clarity and practical implementation. Importantly, the framework here extends that approach by jointly identifying the same structural shocks across both the trend and cyclical components. Maffei-Faccioli (2025) motivates his (trend) identification assumptions through a stylized Keynesian

endogenous growth model with nominal wage rigidities, building on the theoretical foundations of Benigno and Fornaro (2018) and Fornaro and Wolf (2023).

4. Results: Dynamics and Drivers of the EA Inflation Trend and Cycle

This section presents the main empirical results obtained from the estimated model. First, I examine the dynamics of the model's latent states by plotting the evolution of potential GDP, trend inflation, and the output and inflation gaps for the euro area since 1990. Second, I quantify the contribution of structural shocks—both permanent and transitory—in explaining the historical and recent behavior of euro area inflation. This is done through a historical decomposition that traces the impact of each structural shock at time t.

4.A. Hidden Components, Trends and Cycles

Figures 1 and 2 display the estimated low- and high-frequency components of inflation and GDP alongside the observed data. The trend components are shown in the first row and the cyclical components in the second. Red solid lines indicate the observed data, while the thick black lines represent the pointwise median estimates of the trend and cycle components, accompanied by 68% credible intervals.

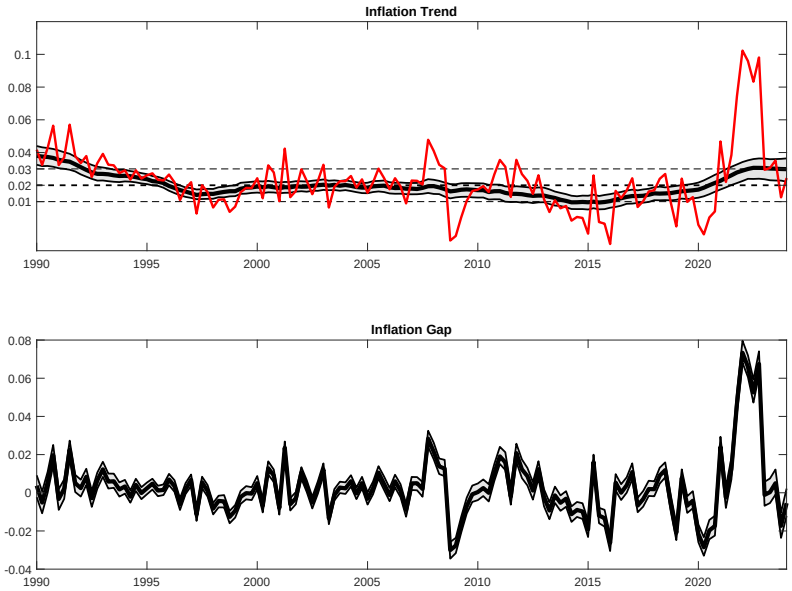

Figure 1. Actual data and estimated trends and cycles of HICP inflation

Note: Point-wise median (solid black line) with 68% credible bands are based on 150000 draws. HICP is defined in annualized quarter-on-quarter terms.

Inflation (Trend Inflation & Inflation Gap). Figure 1 shows substantial fluctuations in the estimated pointwise median of trend inflation over the sample period, which can be divided into five distinct phases: (1) *Early 1990s Decline:* In the early 1990s, estimated trend

inflation declined by more than 200 basis points, falling from approximately 4% to 2% by 1995. (2) *Anchored Period (1995–2012Q3):* Following this decline, trend inflation remained anchored around the 2% level for nearly two decades. This period is characterized by low variability in the trend estimates, consistent with well-anchored inflation expectations. (3) *European Sovereign Debt Crisis (2012–2015):* During the crisis, the median estimate of trend inflation declined by over 100 basis points, reaching a historical low of 1% in 2015Q1. (4) *Post-Crisis Recovery:* After 2015, trend inflation gradually re-anchored near the 2% level. (5) *Post-COVID Economic Reopening:* In the aftermath of the COVID-19 economic reopening, trend inflation rose above the 2% threshold, reflecting renewed inflationary pressures. Finally, as a validation exercise, I assess whether the estimated trend behaves like medium- to long-term inflation expectations by comparing it with euro area market-based inflation compensation at 5-, 10-, and 20-year horizons (not included in the estimation); the series comove closely; see Figure 11 in Appendix C.

The first two findings are consistent with the prevailing view that inflation expectations remained firmly anchored around the 2% level, largely due to the strong credibility of the ECB's price stability mandate (see Altissimo et al. (2006); Bowles et al. (2007); Gorter et al. (2008)). However, the estimated decline in trend inflation between 2012 and 2016 is more contested. While several studies find limited evidence of de-anchoring during this period (see Strohsal and Winkelmann (2015); Jarociński and Lenza (2018); Dovern et al. (2020)), this paper supports a gradual de-anchoring process beginning in 2012, as documented by Gimeno and Ortega (2016); Łyziak and Paloviita (2017) and more recently by Corsello et al. (2021).

In addition, the post-2020 rise in euro area trend inflation documented here has not yet been explored in the literature. The estimates suggest that medium-term inflation is expected to remain above the ECB's target, stabilizing around 3%. This pattern is consistent with the ECB's evolving communication: while in 2021Q4 inflation was described as "temporary and driven largely by transitory factors," by 2022Q4 the ECB projected a more gradual return to target—expecting headline inflation to fall from 8.4% in 2022 to 2.3% in 2025, reaching the 2% target only in the second half of that year.[38]

The lower panel, which displays the inflation gap, shows values around 6–7% during the recent inflation surge. This implies that approximately 85% of the increase in inflation can be attributed to transitory factors. Consistent with this interpretation, Figure 26 in Appendix C shows a sharp rise in the volatility of the inflation gap during this period, reflecting large transitory disturbances driving the post-COVID inflation dynamics. Notably, by 2023Q3, HICP inflation had declined to between 2% and 3%, coinciding with a negative inflation gap. This negative inflation gap likely reflects underlying slack in the economy, as evidenced by the negative output gap shown in the lower panel of Figure 2.

GDP (Potential GDP & Output Gap). Figure 2 shows the pointwise median estimates of potential GDP and the corresponding output gap over the sample period. Two distinct growth

[38] See ECB (2021, 2022).

patterns in potential GDP are evident. (1) *Early 1990s to 2005–06:* During this phase, potential GDP exhibited robust growth, averaging 0.5% quarter-on-quarter (Q-Q). (2) *Post-2007 Slowdown:* From 2007 onward, potential GDP growth experienced a marked deceleration, where the average growth rate declined to 0.24% Q-Q. Even when excluding major crisis episodes such as the Great Financial Crisis (GFC), the European Sovereign Debt Crisis, and the COVID-19 pandemic, trend GDP growth remained subdued at approximately 0.34% Q-Q. This slowdown is consistent with the 'secular stagnation' hypothesis of Ball (2014); Fernández-Villaverde et al. (2013); Gordon (2014); Summers (2014); Gordon (2015), who document a persistent reduction in output growth across advanced economies following the mid-2000s.[39]

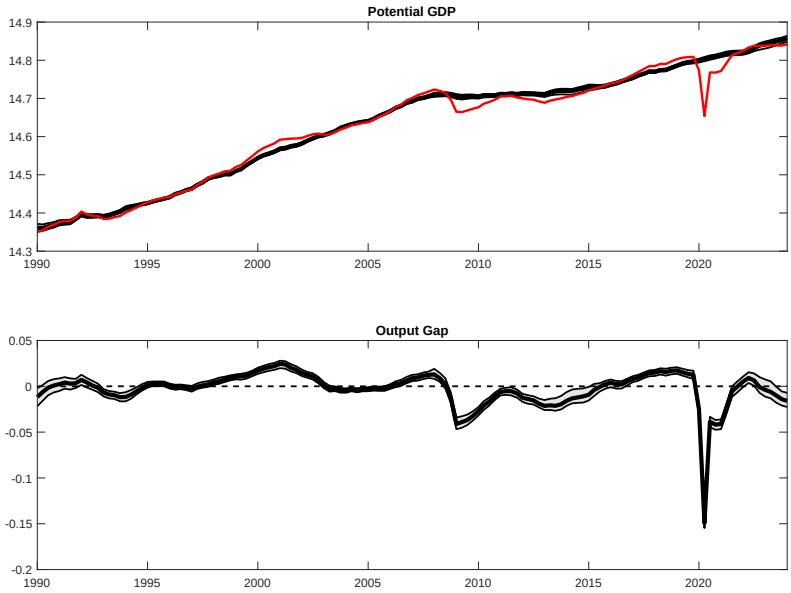

Figure 2. Actual data and estimated trends and cycles of real GDP

Note: Point-wise median (solid black line) with 68% credible bands are based on 150000 draws. Real GDP is defined in log terms.

During the COVID-19 pandemic, the model suggests that potential GDP remained relatively stable, indicating that the underlying productive capacity was not severely impaired. One likely explanation for this resilience is the rapid implementation of supportive policies aimed at mitigating the economic fallout from lockdowns. Several studies (e.g., Bodnár et al. (2020); Blanchard et al. (2020); Bénassy-Quéré et al. (2020)) highlight the importance of liquidity support measures—particularly those that temporarily shifted labor costs from firms to governments—in preventing widespread financial distress and preserving production capacity. By contrast, the lower subfigure shows a sharp decline in the output gap, which reached –14.7% during the lockdown period. This substantial negative gap reflects the sudden and severe contraction in economic activity relative to potential. The increase in macroeconomic

[39] Figure 12 in Appendix C presents the average quarterly growth rate of euro area potential GDP (pointwise median) using five-year rolling windows. The figure shows a clear and sustained decline in trend growth beginning after 2005–06. This pattern is consistent with recent evidence documenting a slowdown in long-term U.S. output growth (see Antolin-Diaz et al. (2017) and Maffei-Faccioli (2025)). The latter study specifically attributes this deceleration to permanent demand-side shocks that began affecting GDP growth after 2000.

volatility is also evident in the heightened variability of the output gap, as shown in Figure 26 in Appendix C.[40]

Finally, Figure 13 in Appendix C illustrates why allowing for time-varying volatility and fat-tailed shocks matters for estimating unobserved components such as potential output and the output gap. The figure reports a decomposition of real GDP from a specification that excludes both stochastic volatility and fat tails. In that homoskedastic model, the pandemic contraction is mechanically spread across the trend and cyclical components, yielding a less credible separation between potential output and the output gap. As a result, estimated potential output becomes more unstable and sensitive to extreme observations.

4.B. Historical Decomposition of euro area Inflation

This subsection presents a historical decomposition of euro area inflation, analyzing the contributions of structural shocks to both trend inflation—driven by permanent shocks—and the inflation gap—shaped by transitory shocks.

Permanent factors driving trend inflation. Figure 3 shows the estimated historical decomposition of the pointwise median of trend inflation—the component labeled as permanent shocks in Equation 9. The colored bars represent the cumulative contribution of each structural shock—domestic (both demand and supply), global (demand and supply), and energy supply—over the period from 1990Q2 to 2024Q1, measured as deviations from the baseline of 1990Q1.[41] The pointwise median of trend inflation is plotted alongside these contributions, offering insight into the evolution of its underlying drivers over time. Figure 15 in Appendix C presents the same decomposition, with both the structural contributions and the pointwise median expressed as deviations from 1990Q1.

Over the full sample period, global and domestic factors account for the majority of the variation in trend inflation, while energy supply shocks play a relatively modest role. However, the relative importance of these five structural shocks in explaining trend inflation evolves considerably over time.

In the early and late 1990s, domestic supply-side factors played a central role in driving trend inflation downward. These negative contributions, alongside more modest negative effects from domestic demand and global supply and demand shocks, accounted for much of the disinflation observed during this period.

In the early 2000s, this disinflationary pressure began to moderate, as the negative contributions from domestic and global supply-side factors were offset by a growing influence of domestic demand shocks and a diminishing negative impact from global demand shocks, follow-

[40] For example, the estimated stochastic volatility of the euro area output gap successfully captures both the increase in volatility during the GFC and the spike observed during the COVID-19 crisis, despite being inferred from a latent variable. This is a notable result, as both the output gap and its volatility are unobserved components jointly estimated by the model.

[41] Figure 14 in Appendix C displays the structural shocks affecting changes in the pointwise median of trend inflation, without accumulation.

ing a sequence of positive surprises—see Figure 14 in Appendix C. By 2006–07, global demand shocks were contributing positively to trend inflation. The interaction of these forces resulted in a prolonged period of stability, with trend inflation anchored around the 2% level.[42]

Following the 2008 financial crisis, the figure reveals a sequence of negative shocks originating from both domestic and global sources. Domestic and global demand shocks began to unwind, exerting downward pressure on trend inflation. Notably, the contribution of global demand shocks turned negative after 2010. These effects were partially offset by a series of negative supply shocks, which tended to raise trend inflation. During this period, energy supply shocks contributed marginally to upward pressure, particularly in response to the sharp increase in oil prices during 2007–08. Nevertheless, the de-anchoring of trend inflation from 2% to 1% was primarily driven by a persistent sequence of negative demand-side shocks, as further illustrated in Figure 4.

In the post-2019 period, the onset of the COVID-19 pandemic led to a rise in trend inflation, primarily driven by supply-side factors—domestic and global—and, to a lesser extent, by demand-side forces. In the historical decomposition, the contribution of domestic and global supply shocks becomes rapidly less negative (i.e., the earlier disinflationary supply contribution unwinds), which mechanically raises the level of trend inflation. At the same time, the previously negative contribution from global demand shocks that accumulated after the Sovereign Debt Crisis also begins to reverse following a sequence of positive global demand shocks. These dynamics are examined in greater detail in Figure 5.

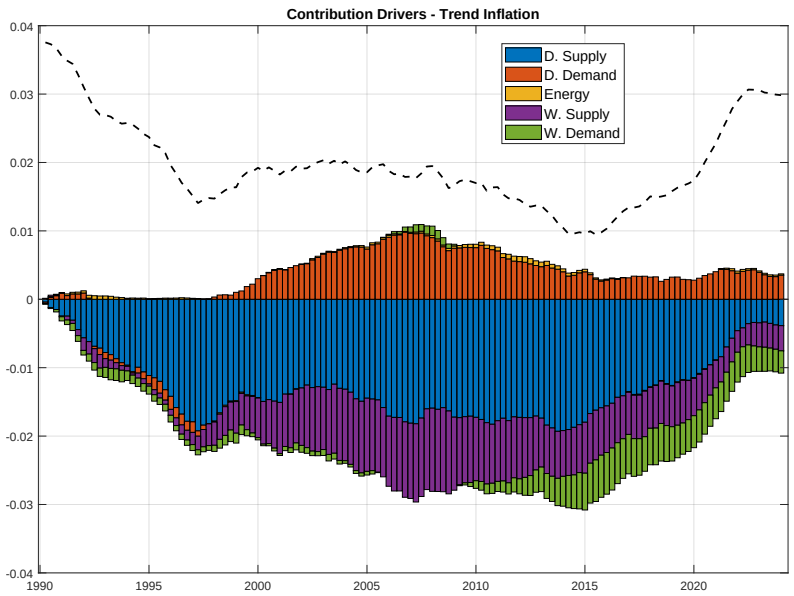

Figure 3. Estimated historical decomposition of the point-wise median of trend inflation from 1990Q2 to 2024Q1

Note: The black line represents the pointwise median of trend inflation, while the colored bars show the cumulative contribution of each structural shock—domestic (demand and supply), global (demand and supply), and energy supply—at time t, measured as deviations from the baseline period of 1990Q1.

[42] As noted by Borio and Filardo (2007) and Bianchi and Civelli (2015), globalization helped reduce inflationary pressures in many advanced economies, including the euro area, prior to the GFC.

The episode of missing inflation in the euro area appears to support explanations that are primarily demand-driven, involving both domestic and global sources.[43] To better understand the role of demand shocks during this period, Figure 4 presents the cumulative contribution of structural shocks starting in 2008.[44]

Trend inflation begins to gradually decline from the 2% level after 2008, largely due to the increasing impact of negative demand shocks—both domestic and global. This downward trend accelerates notably after 2013. Although a series of negative global supply shocks exerted upward pressure on trend inflation in the aftermath of the GFC, the cumulative negative contribution of demand shocks outweighed these supply-side effects. The upward pressure from global supply shocks can be attributed to higher trade costs, fragmentation, and disruptions in global value chains following the financial crisis. This supply-side effect partially offset the disinflationary forces typically associated with globalization (see Bianchi and Civelli (2015); Auer et al. (2017); Forbes (2019); Ha et al. (2019)).

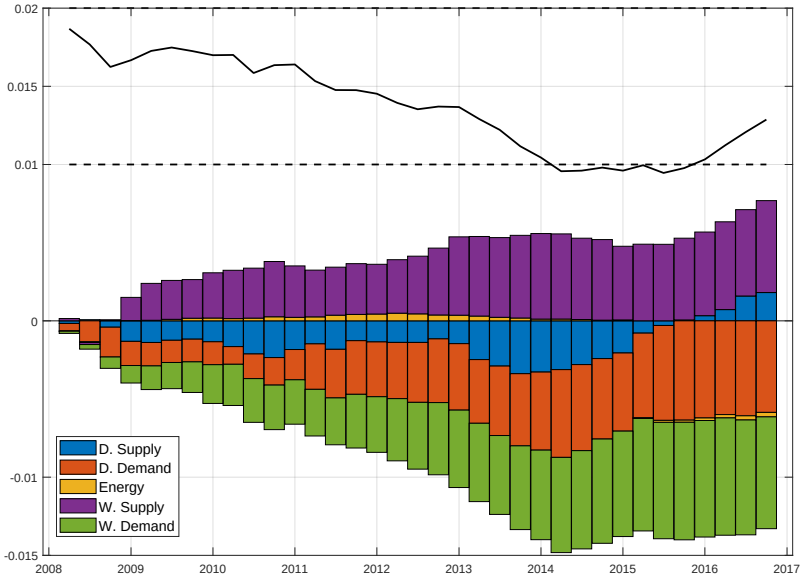

Figure 4. Estimated historical decomposition of median trend inflation from 2008 to 2017

Note: The black line represents the pointwise median of trend inflation, while the colored bars show the cumulative contribution of each structural shock—domestic (demand and supply), global (demand and supply), and energy supply—at time t, measured as deviations from the baseline period of 2008Q1.

The right panel of Figure 16 in Appendix C shows that demand shocks account for approximately 60% of the fluctuations in trend inflation during this period. Notably, domestic demand shocks dominate in the early years, while global demand shocks become the primary demand driver from 2011 onward. These findings align with narratives in the existing literature

[43] See IMF (2016, 2017).

[44] Figure 16 in Appendix C shows, on the left, the historical decomposition of structural shocks and the pointwise median of trend inflation, with all values expressed as deviations from 2008Q1. The right panel displays the same decomposition but normalizes the total contribution of shocks to sum to one at each point in time. This normalization facilitates a clearer visual assessment of which structural shock is contributing most to the variable of interest—trend inflation in this case—by expressing each contribution in percentage terms rather than absolute magnitudes, which can vary over time.

that emphasize the role of demand-side forces in explaining the period of missing inflation (see Ferroni and Mojon (2014, 2017); Conti et al. (2017); Ciccarelli et al. (2017); Bobeica et al. (2019)). However, my results underscore that demand shocks primarily affected the persistent component of inflation, in contrast to the predominantly transitory effects suggested by much of the previous literature.

The recent period following the COVID-19 economic reopening is characterized by a significant surge in trend inflation, largely driven by a combination of supply-side shocks—domestic, and global. Figure 5 illustrates the cumulative contribution of structural shocks beginning in 2019Q4.[45]

The predominance of supply shocks—particularly domestic supply shocks—is evident during this period and can be linked to widespread disruptions in both global and domestic supply chains.[46] Interestingly, the sharp rise in global wholesale energy prices following the COVID-19 crisis, and the subsequent escalation triggered by the Russian invasion of Ukraine, does not appear to have significantly affected the persistent component of inflation.

The role of supply-side drivers in the recent inflation surge is now well-documented. For example, Ascari et al. (2024a), Arce et al. (2024), and Banbura et al. (2023) emphasize how persistent supply-chain disruptions, bottlenecks in industrial goods, and shortages of critical inputs (e.g., semiconductors) have fueled price pressures in the euro area. In contrast, my framework allocates most of the persistent component of inflation to supply disturbances, whereas in their models, supply shocks predominantly drive inflation from a purely deterministic component—essentially an inflation gap.

The divergence in findings can be partly attributed to differences in model specifications. When imposing a deterministic trend, slow-moving dynamics are omitted, causing persistent supply shocks to be absorbed into the cyclical component, making them appear as the dominant drivers of the inflation gap. In my approach, however, the persistent component is modeled as stochastic, allowing the inflation gap to be primarily driven by demand shocks, as illustrated in Figure 6.

To empirically highlight this distinction, I estimate a standard Bayesian VAR model that identifies the same set of structural shocks as in the main model.[47] Figure 29 (Appendix C)

[45] Figure 17 in Appendix C shows, on the left, the historical decomposition of structural shocks and the pointwise median of trend inflation, with all values expressed as deviations from 2019Q3. The right panel displays the same decomposition but normalizes the total contribution of shocks to sum to one at each point in time. This normalization facilitates a clearer visual assessment of which structural shock is contributing most to the variable of interest by expressing each contribution in percentage terms rather than absolute magnitudes, which can vary over time.

[46] Figure 18 reports the uncertainty surrounding the estimated structural contributors, since 2019Q4.

[47] All variables listed in Table 1 enter the model in first differences. The prior for the VAR parameters follows a standard Minnesota prior, with the hyperparameter for overall tightness set to the conventional value of 0.2 (Giannone et al., 2015). However, unlike the standard Minnesota prior, the prior for the "own-lag" parameter is centered at 0 rather than 1, as all variables are specified as stationary processes. The prior variance is specified as an uninformative inverse Wishart distribution, centered at a diagonal matrix of the standard deviations of the error terms from AR(1) regressions for each variable. Degrees of freedom are set to $(n + 2)$, ensuring a well-defined prior mean. The model estimation is based on 30,000 simulations, with the first 10,000 discarded as

presents the historical decomposition of inflation under this specification, while Figure 30 (Appendix C) displays the same decomposition with shocks expressed as relative shares over time. Under this framework, aggregate supply shocks—including domestic, global, and energy supply shocks—account for approximately 60% of the variation in inflation relative to its deterministic component, after 2020.

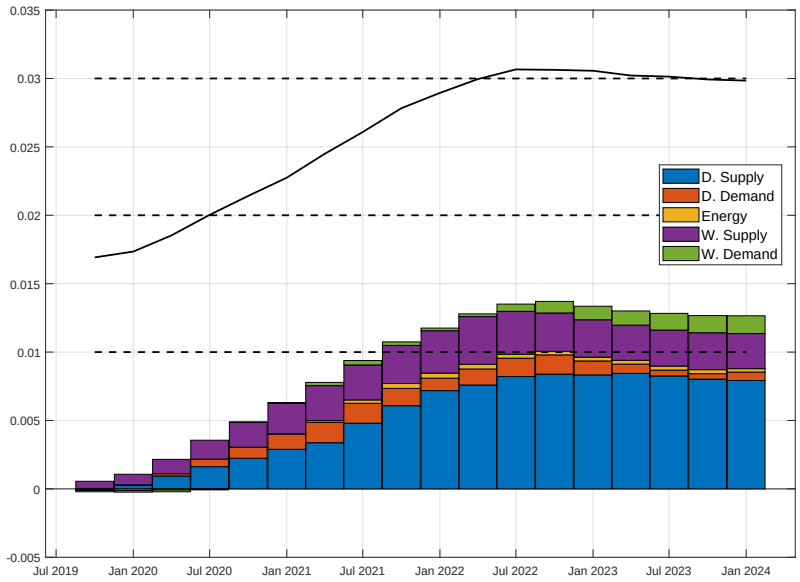

Figure 5. Estimated historical decomposition of median trend inflation from 2019 to 2024

Note: The black line represents the pointwise median of trend inflation, while the colored bars show the cumulative contribution of each structural shock—domestic (demand and supply), global (demand and supply), and energy supply—at time t, measured as deviations from the baseline period of 2019Q3.

Transitory factors driving inflation-gap. Figure 6 illustrates the estimated historical decomposition for the point-wise median of the inflation-gap. The colored bars represent the estimated contribution of each structural shock at each point in time, including domestic shocks (both demand- and supply-side), global shocks (demand- and supply-side), and energy supply shocks over the period from 1990Q2 to 2024Q1. The historical decomposition is computed by drawing from the posterior distribution of all model parameters, constructing the distribution of the historical decompositions, and then taking the pointwise median contribution of each shock, as in Bergholt et al. (2024b). This approach ensures that uncertainty in the estimated VAR parameters is treated symmetrically, as suggested by Bergholt et al. (2024a).

Starting with the GFC, the observed deflation—evidenced by a sustained negative inflation gap—has been largely driven by global factors and domestic demand. Together, global supply and demand shocks explain over 60% of the inflation-gap dynamics that underpinned the post-2007 disinflation. On the supply side, intensified international competition and falling commodity and intermediate-goods prices compressed traded-goods inflation; on the demand side, a synchronized pullback in household and business spending—triggered by financial instability and tighter credit—further dampened aggregate price pressures (Ciccarelli and Mojon (2010),

burn-in draws. Every 10th draw is saved to mitigate potential autocorrelation across draws.

Guerrieri et al. (2010), Mumtaz and Surico (2012), Henriksen et al. (2013), and Ferroni and Mojon (2017)). The relative share of each shock over time is illustrated in Figure 21 (Appendix C).

The low inflation period from the European Sovereign Debt Crisis through 2015 can be attributed to a broader set of shocks, initially driven by demand-side factors and later by supply-side forces, which began to exert a more pronounced effect on the inflation gap. This period reflects the impact of austerity policies and fiscal tightening measures implemented across euro area economies. From 2013 to 2015, the significance of domestic supply shocks increased markedly, accounting for nearly 40% of the variation in the inflation gap, as shown in Figure 21 in Appendix C. This likely reflects constraints in productive capacity and a reduction in public and private sector spending due to fiscal consolidations within the euro area. The prominent role of domestic factors during this period is also highlighted by Bobeica and Jarociński (2019).

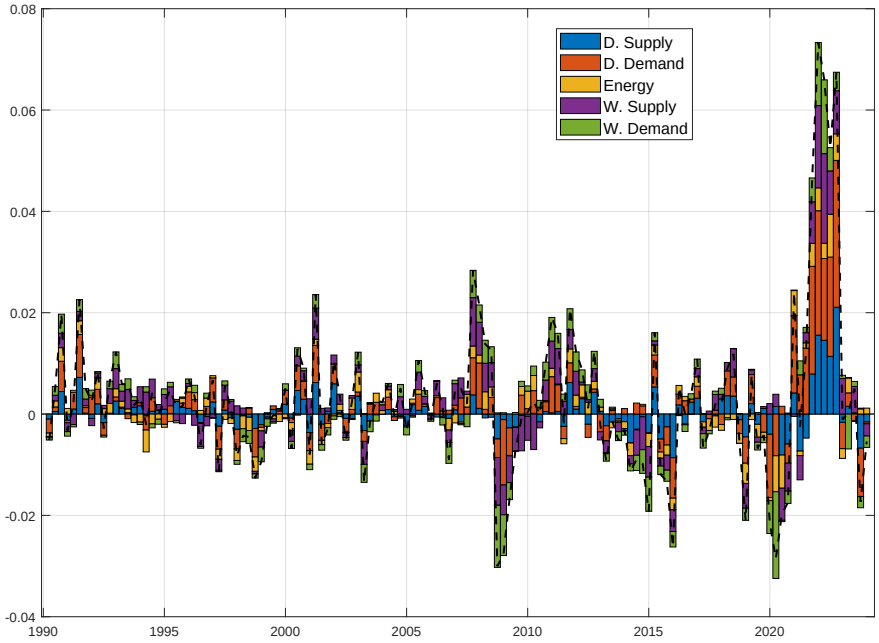

Figure 6. Estimated historical decomposition of the point-wise median of inflation-gap from 1990Q2 to 2024Q1

Note: The black line is the point-wise median of inflation-gap. The colored bars represent the contribution of each structural shock—domestic (demand and supply-side), global (demand and supply-side), and energy supply shocks—at time t.

The COVID-19 pandemic and its aftermath introduced a notable shift in inflation dynamics. Model estimates indicate that recent inflationary episodes have been predominantly driven by transitory factors, which account for approximately 85% of the inflation surge. Specifically, domestic and global demand shocks are the primary contributors to fluctuations in the inflation gap, followed by supply shocks (both domestic and global), while energy supply shocks play a relatively modest role. During this period, demand shocks (domestic and global) explain roughly 70% of the total variance in the inflation gap, as illustrated in Figure 21 in Appendix C.

Moreover, as discussed in the following subsection, these strong transitory effects in domestic demand are also supported by a positive contribution of domestic demand to the output gap.

The demand-driven surge emerged as economies reopened and pandemic-related restrictions were relaxed beginning in 2021Q2. While the paper does not attempt to further disentangle the underlying drivers of these aggregate demand effects (domestic and global), plausible contributors include pent-up consumption, expansive fiscal support (e.g., job-retention schemes), and accommodative monetary policy—operating at both the domestic and international level.

These findings align with recent research by Giannone and Primiceri (2024), who also identify demand-driven factors as the primary drivers of post-pandemic inflation in both the euro area and the United States. At the euro area level, Ascari et al. (2024b) further emphasize the role of fiscal stimulus, highlighting its substantial impact on domestically-driven measures of inflation.

4.C. Historical Decomposition of euro area GDP

This subsection presents a historical decomposition of the structural sources influencing euro area potential GDP—driven by permanent shocks—and the output gap—shaped by transitory shocks.

Permanent factors driving potential GDP. Figure 7 presents the estimated historical decomposition of the pointwise median of potential GDP, excluding the cumulative contribution of the drift term $\bar{c}$. The colored bars represent the cumulative contribution of each structural shock—domestic (both demand and supply), global (demand and supply), and energy supply—over the period from 1990Q2 to 2024Q1, expressed as deviations from the baseline period of 1990Q1. The cumulative contributions are shown on the left axis, while the pointwise median of potential GDP is expressed in logarithmic terms, on the right axis.[48]

It is important to note that, in the absence of shocks, potential GDP grows at a constant rate $\bar{c}$ (see Equation 2). Accordingly, if no structural shocks occur, the pointwise median of potential GDP should follow a linear trajectory. Any deviation from this behavior reflects the influence of shocks to the trend, which generate either positive or negative hysteresis effects. In other words, the constant growth of potential GDP driven by $\bar{c}$ can be either accelerated or decelerated at time t as a result of these shocks.[49]

In the first part of the sample (pre-GFC), shocks made a positive contribution to potential GDP growth, with global supply factors playing a dominant role in explaining long-run fluctuations, followed by domestic demand shocks through 2007. Global demand factors also played an important role, shifting from a sizable negative contribution in the late 1990s to a positive one by 2006–07, driven by a sequence of positive shocks—see Figure 19 in Appendix C.

[48] Figure 19 in Appendix C displays the structural shocks affecting changes in the pointwise median of potential GDP, excluding the drift term $\bar{c}$.

[49] For instance, Bluedorn and Leigh (2019) provide evidence of positive hysteresis in 34 advanced economies, where permanent reductions in unemployment are associated with prolonged periods of economic expansion. Conversely, Furlanetto et al. (2025) find evidence of negative hysteresis, showing that negative permanent demand shocks significantly affect the U.S. economy, leading to lasting declines in employment and investment.

Following the 2008 financial crisis, there is a notable de-accumulation in the contribution of structural shocks. From 2008 onward, potential GDP growth appears to be sustained almost entirely by the drift component $\bar{c}$, until 2022Q4, when the net contribution of shocks turns slightly positive again—resembling the pre-GFC period. This result helps explain why average potential GDP growth was stronger during 1990–2007 (0.50% Q-Q) compared to the post-2008 period (0.34% Q-Q), even when excluding the most severe episodes of the GFC, the European Sovereign Debt Crisis, and the COVID-19 pandemic.

These findings suggest a structural shift in the underlying forces driving potential GDP in the euro area following the 2008 financial crisis. The pre-GFC period is marked by a steady accumulation of positive contributions from global supply shocks, domestic demand shocks, and the drift term $\bar{c}$, supporting sustained potential GDP growth. In contrast, the post-GFC period is characterized by a negative accumulation of all shocks—primarily global—which exerts persistent downward pressure on potential output. In fact, the previously positive contribution of global demand shocks in 2006–07 turns negative shortly thereafter, reflecting a structural change in the dynamics of globalization.

This latter result aligns with the theory of the "great trade collapse," which posits that the synchronized contraction in global trade in late 2008—driven largely by the postponement of purchases, particularly of durable consumer and investment goods—resulted in permanent output losses globally.[50]

Another factor contributing to the decline in potential GDP is the negative impact of energy supply shocks following the GFC, which accounted for nearly one percentage point of the total decline and began to converge toward zero from 2013 onward.[51]

With the onset of the COVID-19 pandemic, the contribution of global and domestic shocks continued to decline, with global supply and domestic supply and demand shocks becoming less influential—particularly the former. In addition, the influence of energy supply shocks increased after 2021, accounting for approximately half a percentage point of the total decline in potential GDP. This renewed contribution is tied to the global surge in wholesale energy prices following the COVID-19 pandemic and the onset of the Russian invasion of Ukraine—see the negative shocks in 2022Q1–Q2 in Figure 19 in Appendix C.

After 2022Q3, the contribution of global shocks begins to recover, driven in part by a sequence of positive global demand shocks that gradually reduce their earlier negative impact. As a result, the net contribution of shocks to potential GDP turns positive again. Finally,

[50]For evidence that the collapse was primarily demand-driven, see Baldwin (2009), Levchenko et al. (2010), Abiad et al. (2014), and Chen et al. (2019). Other studies emphasize the role of global supply-side disruptions, often in conjunction with global demand shocks—see Alessandria et al. (2010), Chor and Manova (2012), Bems et al. (2013), and Eaton et al. (2016).

[51]This timing coincides with the major expansion of oil and gas fracking between 2012 and 2014, during which global oil prices fell sharply due to the surge in U.S. shale oil production.Between June 2013 and January 2016, global oil prices declined by approximately 70%. Brent crude oil, which was trading at around $115 per barrel in mid-2014, fell to about $30 per barrel by early 2016. For more on the effects of fracking on economic growth, see Hausman and Kellogg (2015) and Gilje et al. (2016).

consistent with Giannone and Primiceri (2025), the model identifies strong post-pandemic demand; in the decomposition, domestic demand shocks through 2021-2022 and global demand shocks from 2023 onward contribute positively to the estimated potential GDP. Figure 20 in Appendix C plots the cumulative contribution of structural shocks and the drift. It shows that since 2020, domestic and global demand shocks have been the only structural innovations to drive potential GDP above its underlying drift. Given the observed path of actual GDP, this rise in estimated potential GDP mechanically implies that the estimated output gap becomes negative after 2022-2023—a pattern whose structural drivers are examined in detail in the following subsection.

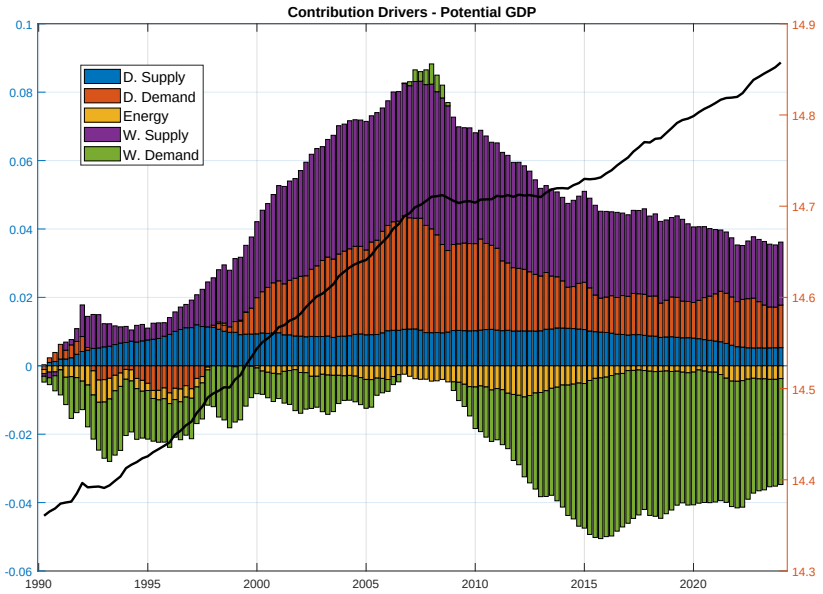

Figure 7. Estimated historical decomposition of the pointwise median of potential GDP, excluding the cumulative contribution of the drift term $\bar{c}$, from 1990.Q2 to 2024.Q1

Note: The black line is the point-wise median of potential GDP is expressed in logarithmic terms, on the right axis. The colored bars show the cumulative contribution of each structural shock—domestic (demand and supply), global (demand and supply), and energy supply—at time t, measured as deviations from the baseline period of 1990.Q1.

Transitory factors driving output-gap. Figure 8 illustrates the estimated historical decomposition for the point-wise median of the output-gap. The colored bars represent the estimated contribution of each structural shock at each point in time, including domestic shocks (both demand- and supply-side), global shocks (demand- and supply-side), and energy supply shocks over the period from 1990Q2 to 2024Q1. The historical decomposition is computed by drawing from the posterior distribution of all model parameters, constructing the distribution of the historical decompositions, and then taking the pointwise median contribution of each shock, as in Bergholt et al. (2024b). This approach ensures that uncertainty in the estimated VAR parameters is treated symmetrically, as suggested by Bergholt et al. (2024a). va The Financial Crisis and the European Sovereign Debt Crisis are characterized by distinct factors driving economic activity during these periods. The sharp contraction in economic activity between

2008–09 is predominantly explained by global factors, which account for approximately 60% of the output gap fluctuations; nonetheless, domestic demand also played a significant role in driving the downturn. In contrast, the downturn between 2012-15 is driven more by domestic and energy factors, with around 50% of the output gap variation explained by domestic supply and energy supply shocks. See Figure 22 in Appendix C, which plots the relative importance of each shock from a historical perspective.

The COVID-19 lockdown resulted in a significant negative output gap, as indicated by the model estimates. While it is difficult to provide a definitive economic interpretation for the magnitude of this decline, a tentative explanation can be inferred from the historical decomposition results. These results suggest that the COVID-19 lockdown shock was multifaceted, driven by both global and domestic factors.[52]

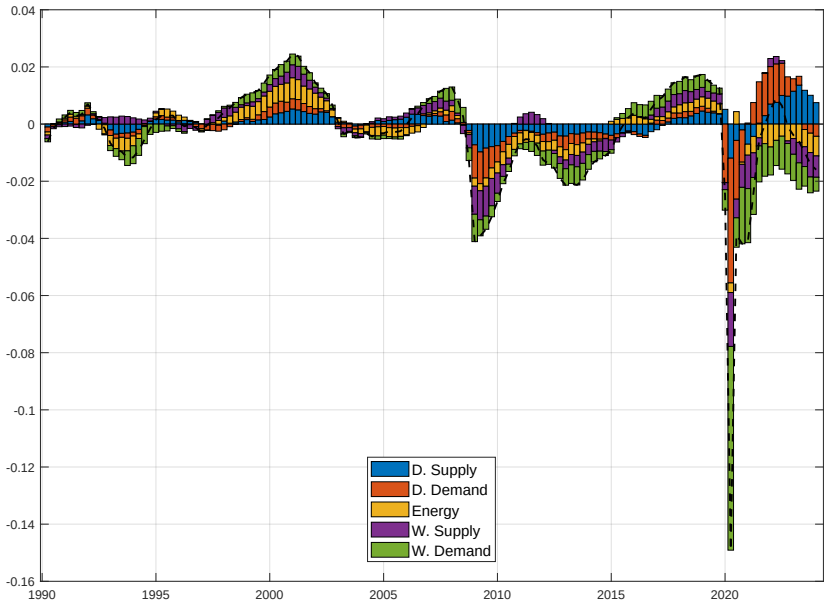

Figure 8. Estimated historical decomposition of the point-wise median of output-gap from 1990.Q2 to 2024.Q1

Note: The black line is the point-wise median of output-gap. The colored bars represent the contribution of each structural shock—domestic (demand and supply-side), global (demand and supply-side), and energy supply shocks—at time t.

The subsequent economic rebound following the reopening is predominantly driven by domestic demand factors, accounting for nearly 90% of the recovery.[53] This finding supports the earlier inflation-gap results and underscores that, in the post-reopening period, demand for goods and services surged. The continuation of the economic recovery after 2023 appears to be primarily driven by positive domestic supply shocks.

Interestingly, energy supply shocks account for roughly one-third of the negative contri-

[52]Similar conclusions are drawn in reports from the ECB and the St. Louis Federal Reserve; see Croitorov et al. (2021), Martin et al. (2022), and Muggenthaler et al. (2021).

[53]ECB policy, as discussed by De Santis and Stoevsky (2023), provides a similar narrative, emphasizing that demand-side forces played a crucial role in driving the post-pandemic recovery in economic activity.

butions to the output gap, beginning with the global surge in wholesale energy prices in the second half of 2021 and intensifying after the onset of the Russian invasion of Ukraine. This observation is also consistent with recent findings by Giannone and Primiceri (2024), who, in their model extensions, identify demand, non-energy supply, and energy supply shocks as key drivers of output fluctuations.

5. Conclusions

Since the post-COVID economic reopening, euro area inflation has surged to a 40-year high, raising significant concerns about its underlying drivers. This paper addresses two central questions: (1) What are the structural channels driving euro area inflation? The analysis disentangles shocks into global and domestic components from both demand and supply perspectives. (2) Do these structural channels primarily affect the transitory component of inflation—the inflation gap—or the persistent component—trend inflation? To address these questions, I employ a novel econometric model that integrates variable decomposition into trends and cycles, incorporates time-varying second moments, and identifies structural shocks.

The findings provide evidence that both domestic supply shocks and demand shocks (domestic and global) have been the primary drivers of the post-COVID inflation surge. However, unlike the existing literature, I find that domestic supply shocks primarily feed into the persistent component of euro area inflation, raising trend inflation to 3% by 2022. In contrast, demand shocks—both domestic and global—manifest primarily in the transitory component (inflation gap), which accounts for approximately 85% of the total post-COVID increase in inflation.

This approach contrasts with conventional VAR frameworks in which inflation is analyzed around a deterministic component. In this paper, the corresponding low-frequency component is instead modeled as a stochastic trend, which allows inflation dynamics to be decomposed into persistent (trend) and transitory (gap) movements.

Furthermore, the paper underscores the importance of modeling time-varying second moments (stochastic volatility and fat tails). In a specification that abstracts from these dynamics, the exceptional COVID-19 collapse in real GDP is mechanically spread across the trend and cyclical components—partly absorbed by potential output and partly by the output gap—thereby overstating the decline in potential GDP. Additionally, the model estimates a significant slowdown in euro area potential GDP growth, with quarter-on-quarter growth declining from an average of 0.50% between the early 1990s and 2005–06 to just 0.24% from 2006 onward. This deceleration is largely driven by global factors, aligning with theories that suggest a permanent structural shift in globalization.

While this paper offers a novel benchmark, it does so at the cost of imposing an independent trend-cycle decomposition. This assumption may limit the model's flexibility in capturing interactions between transitory and permanent shocks. Thus, further work is needed to refine the econometric framework, particularly in the model decomposition and shock identification

scheme. A promising avenue for future research would involve allowing transitory shocks to transmit to the permanent component while retaining time-varying second moments. For instance, a transitory shock could become more persistent—or even permanent—if it activates mechanisms within the model that generate sustained economic disruptions.

A A Gibbs Sampler for a VAR with Common Trends featuring Stochastic Volatility

The VAR with Common Trends and SV with fat-tails specified in equations 1 through 8 is estimated using a Gibbs sampler and Metropolis hasting, which involves the following blocks:

1. The first step requires to set up starting values, $\phi^{\epsilon}_{ij,t}, \phi^{u}_{ij,t}, h^{\epsilon}_{i,t}, h^{u}_{i,t}, \delta_{i,t}$, to form the history of $\Sigma^{\epsilon}_{1:T}, \Sigma^{u}_{1:T}, y_{1:T}$. Draws from the joint distribution $\bar{y}_{0:T}, \tilde{y}_{-p+1:T}, \lambda \mid \text{vec}(\mathcal{A}), \Sigma^{\epsilon}_{1:T}, \Sigma^{u}_{1:T}, y_{1:T}, \text{vec}(\mathcal{V})$, are obtained, which is given by the product of the marginal posterior of $\lambda \mid \text{vec}(\mathcal{A}), \Sigma^{\epsilon}_{1:T}, \Sigma^{u}_{1:T}, y_{1:T}, \text{vec}(\mathcal{V})$ times the distribution of the initial observations $\bar{y}_{0:T}, \tilde{y}_{-p+1:T} \mid \lambda, \text{vec}(\mathcal{A}), \Sigma^{\epsilon}_{1:T}, \Sigma^{u}_{1:T}, y_{1:T}, \text{vec}(\mathcal{V})$. Where, $\text{vec}(\mathcal{V}) = \text{vec}(D^{u}, D^{\epsilon}, G^{u}, G^{\epsilon}, \kappa_{\delta})$. The marginal posterior of $\lambda \mid \text{vec}(\mathcal{A}), \Sigma^{\epsilon}_{1:T}, \Sigma^{u}_{1:T}, y_{1:T}, \text{vec}(\mathcal{V})$ is given by:

$$p\left(\lambda \mid \text{vec}(\mathcal{A}), \Sigma^{\epsilon}_{1:T}, \Sigma^{u}_{1:T}, y_{1:T}, \text{vec}(\mathcal{V})\right) \propto \mathcal{L}\left(y_{1:T} \mid \lambda, \text{vec}(\mathcal{A}), \Sigma^{\epsilon}_{1:T}, \Sigma^{u}_{1:T}, \text{vec}(\mathcal{V})\right) p(\lambda)$$

where $\mathcal{L}\left(y_{1:T} \mid \lambda, \text{vec}(\mathcal{A}), \Sigma^{\epsilon}_{1:T}, \Sigma^{u}_{1:T}, \text{vec}(\mathcal{V})\right)$ is the likelihood obtained by using the Kalman Filter in the state-space model specified in equation (1). Since $p\left(\lambda \mid \text{vec}(\mathcal{A}), \Sigma^{\epsilon}_{1:T}, \Sigma^{u}_{1:T}, y_{1:T}, \text{vec}(\mathcal{V})\right)$ could feature an unknown form, this step involves a Metropolis-Hastings algorithm. Finally, in step 1, I use Carter and Kohn (1994)'s simulation smoother to obtain draws for the trend and cycle components $\bar{y}_{0:T}, \tilde{y}_{-p+1:T}$, for given $\lambda, \bar{c}$ and $\text{vec}(\mathcal{A}), \Sigma^{\epsilon}_{1:T}, \Sigma^{u}_{1:T}, y_{1:T}, \text{vec}(\mathcal{V})$.

2. The second step is standard to the time-series literature because $\bar{y}_{0:T}, \tilde{y}_{-p+1:T}$ are given.

2.a To obtain the time-varying elements of $\Sigma^{u}_{1:T}$, $p\left(\Sigma^{u}_{1:T} \mid \tilde{y}_{1:T}, \bar{y}_{1:T}, \lambda, \bar{c}, \text{vec}(\mathcal{A}), \Sigma^{\epsilon}_{1:T}, y_{1:T}, \text{vec}(\mathcal{V})\right)$, I follow the algorithm described in Primiceri (2005) and Benati and Mumtaz (2007). (i) Compute the VAR residuals, $\hat{u}_t = \tilde{y}_t - \bar{\mathcal{A}}'^{(j-1)}\tilde{x}_t$, where $\bar{\mathcal{A}}'^{(j-1)}$ is the previous of these parameters. Draw the time-varying, $\phi^{u}_{ij,t}$, elements of Φ^{u}_{t} using the Carter and Kohn algorithm (conditional on the previous of these parameters $\bar{\mathcal{A}}, H^{u}_{t}, D^{u}_{1:n}$). Then the state space formulation for $\phi^{u}_{ij,t}$ is derived from the following relationship

$$\begin{pmatrix} 1 & 0 & \dots & 0 \\ \phi^{u}_{21,t} & 1 & \ddots & \vdots \\ \vdots & \ddots & \ddots & 0 \\ \phi^{u}_{k1,t} & \dots & \phi^{u}_{kk-1,t} & 1 \end{pmatrix} \begin{pmatrix} u_{1,t} \\ u_{2,t} \\ \vdots \\ u_{k,t} \end{pmatrix} = \begin{pmatrix} o_{1,t} \\ o_{2,t} \\ \vdots \\ o_{k,t} \end{pmatrix},$$

where, $\text{VAR}(o_t) = H^{u}_{t}$. The state space formulation for $\phi^{u}_{21,t}$ is

$$u^{u}_{2,t} = -a^{u}_{21,t}u_{1,t} + o_{2,t},\ VAR\left(o_{2,t}\right) = h^{u}_{2,t}$$
$$a^{u}_{21,t} = a^{u}_{21,t-1} + V_{1t},\ VAR\left(V_{1t}\right) = D^{u}_{1}.$$

The state space formulation for $a^u_{31,t}$ and $a^u_{32,t}$ is

$$u_{3,t} = -a^u_{31,t}u_{1,t} - a^u_{32,t}u_{2,t} + o_{3,t}, VAR\left(o_{3,t}\right) = h^u_{3,t}$$
$$\begin{pmatrix} a^u_{31,t} \\ a^u_{32,t} \end{pmatrix} = \begin{pmatrix} a^u_{31,t-1} \\ a^u_{32,t-1} \end{pmatrix} + \begin{pmatrix} V_{2t} \\ V_{3t} \end{pmatrix}, VAR \begin{pmatrix} V_{2t} \\ V_{3t} \end{pmatrix} = D^u_2.$$

The same procedure is applied to obtain the rest of the state space formulations. (ii) Conditional on a draw for $(a_{21,t}), (a_{31,t}$ and $a_{32,t}), \ldots, (a_{81,t}, \ldots,$ and $a_{87,t})$ calculate the residuals $(V^u_{1,t}, V^u_{2,t}, \ldots, V^u_{8,t})$. Draw each of D^u_i from the inverse Wishart distribution with scale matrix $V^{\prime,u}_{i,t}V^u_{i,t} + (\kappa + i + 1)\left(\eta_z \underline{D^u_i}\right)$ and degrees of freedom $T + \kappa_{D,u}$; where i = 1, $\cdots$, (n-1), $\kappa_{D,u} = (\kappa + i + 1)$, and κ equals one. (iii) Using the draw of Φ^u_t calculate $o_t = \Phi^u_t u_t$. Notice that, o_t are contemporaneously uncorrelated then drawing $h^u_{i,t}$ and $\delta_{i,t}$ can be done separately by simply applying the independence Metropolis-Hastings algorithm. (iii-A) As in Geweke (1993) I use the Random Walk Metropolis Hastings Algorithm to draw from the following conditional distribution:

$$G(\kappa_{\delta,i}|\Psi) \propto \left(\frac{\kappa_{\delta,i}}{2}\right)^{\frac{T\kappa_{\delta,i}}{2}} \Gamma\left(\frac{\kappa_{\delta,i}}{2}\right)^{-T} \exp\left(-\left(\frac{1}{n_0} + 0.5\sum_{t=1}^{T}\left[\ln\left(\delta^{-1}_{i,t}\right) + \delta_{i,t}\right]\kappa_{\delta,i}\right)\right).$$

More specifically, for each of the n equations of the VAR, I draw $\kappa^{\text{new}}_{\delta,i} = \kappa^{\text{old}}_{\delta,i} + \tilde{c}^{1/2}\tilde{u}$ with $\tilde{u} \sim N(0,1)$. The draw is accepted with probability $\min\left(1, \frac{G(\kappa^{\text{new}}_{\delta,i}|\bar{\delta}_k)}{G(\kappa^{\text{old}}_{\delta,i}|\bar{\delta}_i)}\right)$, where $\bar{\delta}_i = [\delta_{i,1}, \delta_{i,2}, \ldots, \delta_{i,T}]$, with $\tilde{c}$ chosen to keep the acceptance rate around 20-40%. (iii-B) $h^u_{i,t}$ can be done separately by simply applying the independence Metropolis-Hastings algorithm conditional on a draw for g^u_i. This is done using the univariate algorithm by Jacquier et al. (2004). Finally, as discussed in Cogley and Sargent (2005) draw g^u_i (each diagonal element of G^u), conditional on $h^u_{i,t}$, from inverse Gamma distribution with scale parameter

$$\frac{\sum_{t=1}^{T}\left(\ln h^u_{i,t} - \ln h^u_{i,t-1}\right)^2 + g^u_i}{2}$$

and degrees of freedom $\frac{T+\kappa_G}{2}$.

2.b Sampling $\Sigma^{\epsilon}_{1:T}$, $p\left(\Sigma^{\epsilon}_{1:T} \mid \bar{y}_{1:T}, \tilde{y}_{1:T}, \lambda, \bar{c}, \text{vec}(\mathcal{A}), \Sigma^u_{1:T}, y_{1:T}, \text{vec}(\mathcal{V})\right)$ in the trend equation. Given the coefficients $(\bar{c})$ and latent trends $(\bar{y}_{1:T})$, construct the trend innovations $\hat{\epsilon}_t = \bar{y}_t - \bar{c} - \bar{y}_{t-1}$. Then sample the time-varying elements of $\Sigma^{\epsilon}_{1:T}$ by applying the updating steps as in Step 2.a(i), 2.a(ii), and 2.a(iii-B), replacing the cycle residuals with $\hat{\epsilon}_{1:T}$ and setting the dimension to q.

2.c The posterior distribution of $\text{vec}(\bar{\mathcal{A}})$ is given by a Metropolis-Hastings step, as in Del Negro et al. (2019). In this way, this proposal takes into account the conditional initial observations

$\tilde{y}_{0:-p+1}$. The posterior distribution of $\text{vec}(\bar{\mathcal{A}})$ is given by

$$(\bar{\Sigma}^{\mathcal{A}})^{-1} = (\underline{\Sigma_0^{\mathcal{A}}})^{-1} + \sum_{t=1}^{T} \left((\Sigma_t^u)^{-1} \otimes \tilde{x}_t \tilde{x}_t' \right),$$

$$\text{vec}(\bar{\mathcal{A}}) = \bar{\Sigma}^{\mathcal{A}} \left\{ \text{vec} \left(\sum_{t=1}^{T} (\Sigma_t^u)^{-1} \tilde{y}_t \tilde{x}_t' \right) + (\underline{\Sigma_0^{\mathcal{A}}})^{-1} \text{vec}(\underline{\mathcal{A}}) \right\} I(\text{vec}(\underline{\mathcal{A}})),$$

where $\tilde{x}_t = \left(\tilde{y}_{t-1}', \cdots, \tilde{y}_{t-p}' \right)'$ collects the VAR regressors. Finally, a MH step is needed to account for the istribution of $\tilde{y}_{0:-p+1}$, where the acceptance probability is given by:

$$\alpha^{\text{MH}} = \min \left\{ 1, \frac{\text{Num}}{\text{Den}} \right\}$$

, where

$$\text{Num} = \prod_{t=1}^{T} \mathcal{N}(\tilde{y}_{0:-p+1}; 0, V(\text{vec}(\bar{\mathcal{A}})^*, \Sigma_t^*)) \times I(\text{vec}(\bar{\mathcal{A}})^*),$$

and

$$\text{Den} = \prod_{t=1}^{T} \mathcal{N}(\tilde{y}_{0:-p+1}; 0, V(\text{vec}(\bar{\mathcal{A}})^{j-1}, \Sigma_t^{j-1})) \times I(\text{vec}(\bar{\mathcal{A}})^{j-1}),$$

where $\text{vec}(\bar{\mathcal{A}})^\star, \Sigma_t^*$ are current draws, $\mathcal{N}(\mu, V)$ represents the density of the Gaussian distribution with mean μ and variance V, and $\text{vec}(\bar{\mathcal{A}})^{j-1}$ is the previous draw for these parameters. Repeat steps from 1 to 2.c M times. The last L draws provide an approximation to the marginal posterior distributions of the model parameters.

Identification procedure. The identification procedure described in subsection 3.*C* is performed using the algorithm of Arias et al. (2018), which consists of the following steps, for each given draw from the posterior of the reduced-form parameters (permanent side):

Step one. Draw a q x q matrix W from $N(0_n, I_q)$ and perform a QR decomposition of W, with the diagonal of R normalized to be positive and $Q^\epsilon Q^{\epsilon\prime} = I_q$.

Step two. Let S_t^ϵ be the lower triangular Cholesky decomposition of Σ_t^ϵ and define $B_t = S_t^\epsilon Q^{\epsilon\prime}$. Compute the candidate (permanent) responses are given by B_t. Check the set of permanent responses, if it satisfies all the sign restrictions, store them. If not, discard them and go back to the first step.

Step three. Repeat steps 1 and 2 until M impulse responses that satisfy the sign restrictions are obtained. The resulting set characterizes the set of structural VAR models that satisfy the sign restrictions.

The identification procedure for the transitory side is as follows:

Step one. Draw a n x n matrix W from $N(0_n, I_n)$ and perform a QR decomposition of W, with the diagonal of R normalized to be positive and $Q^u Q^{u\prime} = I_n$.

Step two. Let S_t^u be the lower triangular Cholesky decomposition of Σ_t^u and define $C_t^u =$

$S_t^u Q^{u\prime}$. Compute the candidate impulse responses as $IRF_{j,t} = A_j C_t^u$, where A_j are the reduced form impulse responses from the Wold representation, for $j = 0, \ldots, J$. If the set of impulse responses satisfies all the sign restrictions, store them. If not, discard them and go back to the first step.

Step three. Repeat steps 1 and 2 until M impulse responses that satisfy the sign restrictions are obtained. The resulting set characterizes the set of structural VAR models that satisfy the sign restrictions.

B Convergence of the Markov chain Monte Carlo algorithm

This appendix assesses convergence of the Markov chain Monte Carlo algorithm in the baseline application to the euro area data. Following Primiceri (2005), I assess the convergence of the Markov chain by inspecting the autocorrelation properties of the ergodic distribution's draws. In order to judge how well the chain mixes, common practice is to look at the draws' inefficiency factors (IF) for the posterior estimates of the parameters. Specifically, that is the inverse of the relative numerical efficiency measure of Geweke et al. (1991), i.e., the IF is an estimate of $(1 + 2\sum_{i=1}^{\infty} \rho_i)$, where ρ_i is the i-th autocorrelation of the chain. In this application the estimate is performed using a Parzen window.[54] Values of the IFs below or around 20 are regarded as satisfactory, as stressed by Primiceri (2005). Figure 9 plots a complete description of the characteristics of the chain for the different sets of parameters. All the IFs are around or even below 20. $D^{\epsilon}, D^{u}, G^{\epsilon}, G^{u}$: elements of the covariance matrix of the model's innovations; $H_{\epsilon,t}, H_{u,t}$: time varying volatilities from the permanent and transitory side; $\Phi_{\epsilon,t}, \Phi_{u,t}$: time varying simultaneous relations; κ_{δ}: degrees of freedom for the Student's t-distribution; $\mathcal{A}$: time-invariant autoregressive coefficients; Λ: time-invariant cointegrating coefficients; $\bar{c}$: time-invariant drifts.

[54] For inefficiency factors, see Section 6.1 of Giordani et al. (2011).

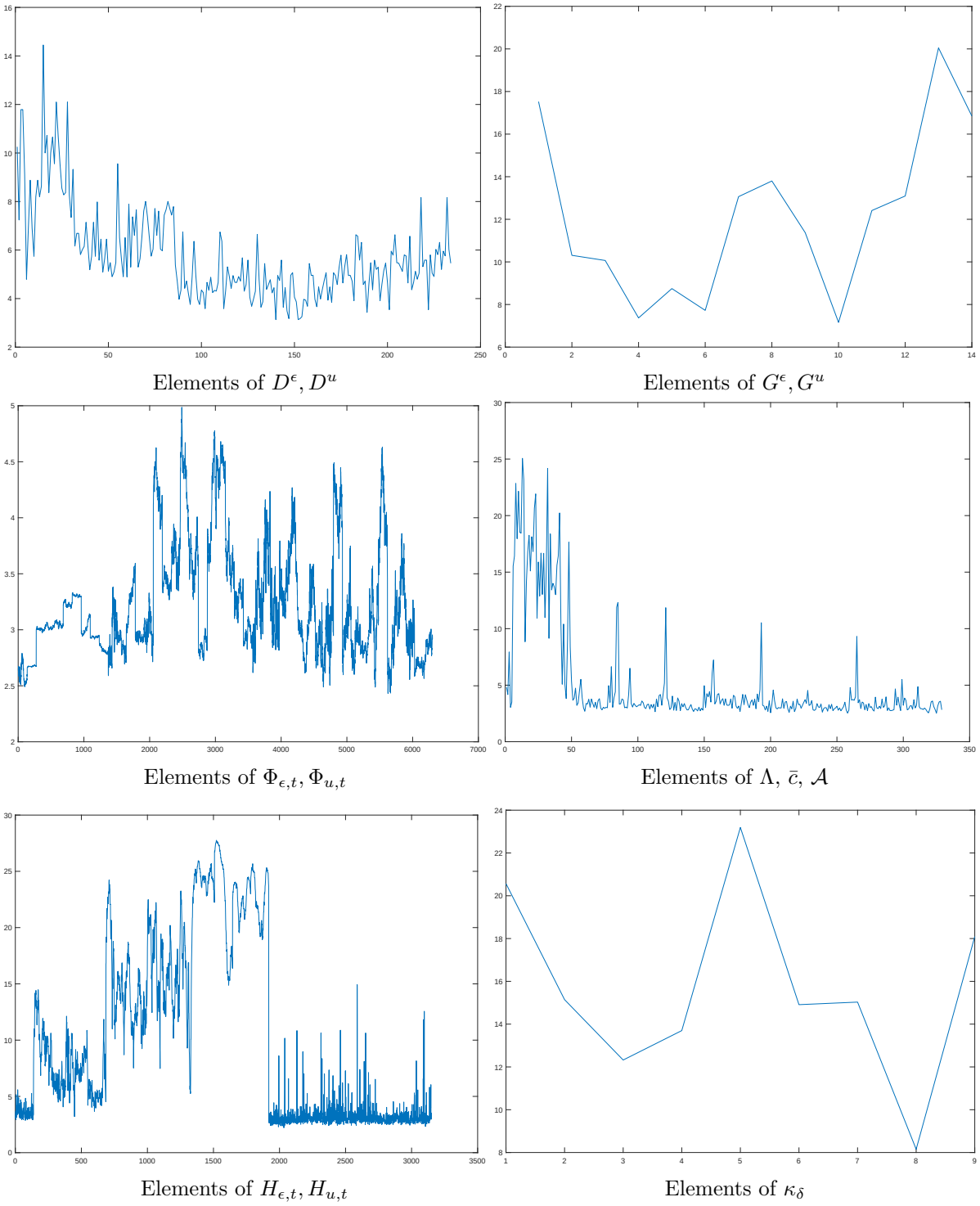

Figure 9. Summary of the distribution of the Inefficiency Factors for different sets of parameters

C Tables and Figures

Table 5. Johansen Cointegration Rank Test Results

NH (H_0)	**AH (H_1)**	**Statistic**	**Critical Value**	***p*-value**	**Decision (5%)**
$r = 0$	$r \geq 1$	55.6178	35.1929	0.0010	Reject H_0
$r \leq 1$	$r \geq 2$	24.4643	20.2619	0.0126	Reject H_0
$r \leq 2$	$r = 3$	7.8494	9.1644	0.0883	Fail to reject H_0

Notes: The trace statistic is used with 5% significance. Model contains intercepts in cointegrating relations, no deterministic trends, and 4 lags are applied. Rejection of H_0 indicates evidence for the alternative hypothesis. Variables: EA HICP Inflation, Price Trends next 12 months, and Unit Labor Cost Index.

Table 6. Augmented Dickey-Fuller Test Results

Variable	**Test Statistic**	**Critical Value**	***p*-value**	**Decision (5%)**
Unemployment Rate	0.6061	-1.9422	0.8465	Fail to reject H_0
Δ Unemployment Rate	-5.9314	-1.9422	0.0010	Reject H_0

Notes: The ADF test is conducted with an AR model and 0 lags. The null hypothesis H_0 is that the series has a unit root (non-stationary). A 5% significance level is used.

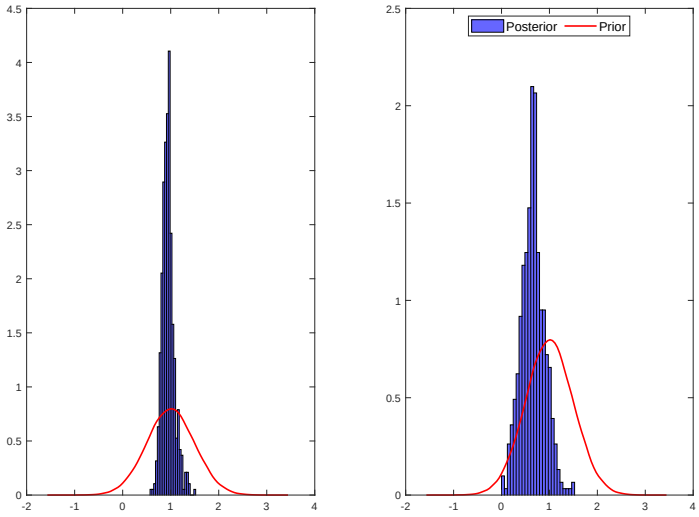

Figure 10. Prior and posterior of Λ

Note: Prior and posteriors distributions of the coefficients λ_1 and λ_2 in Λ

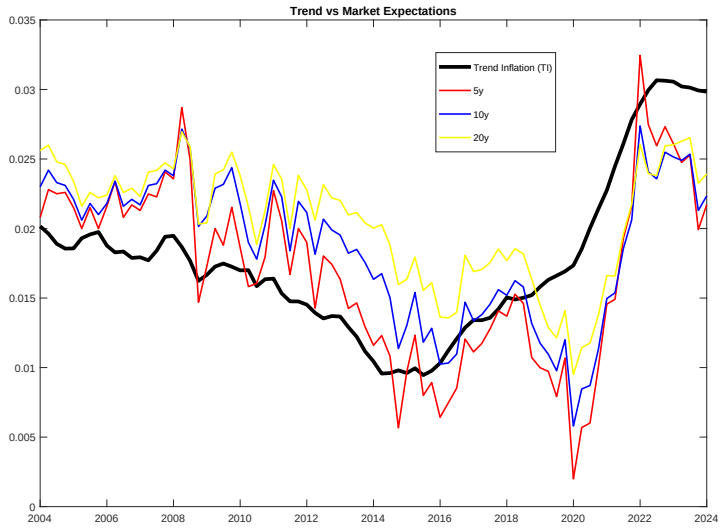

Figure 11. Market inflation swaps: 5, 10 and 20 year and median trend inflation

Note: Source of inflation swaps: Refinitiv.

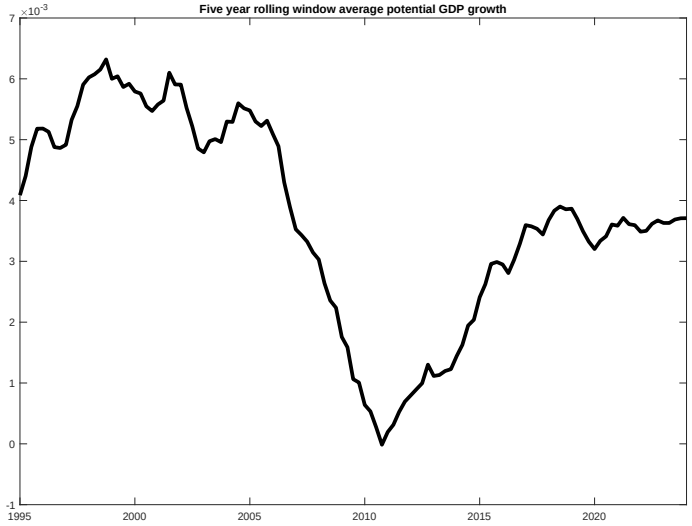

Figure 12. Average quarterly growth rate over five-year rolling windows

Note: Average quarterly growth rate of EA Potential GDP Point-wise median over five-year rolling windows.

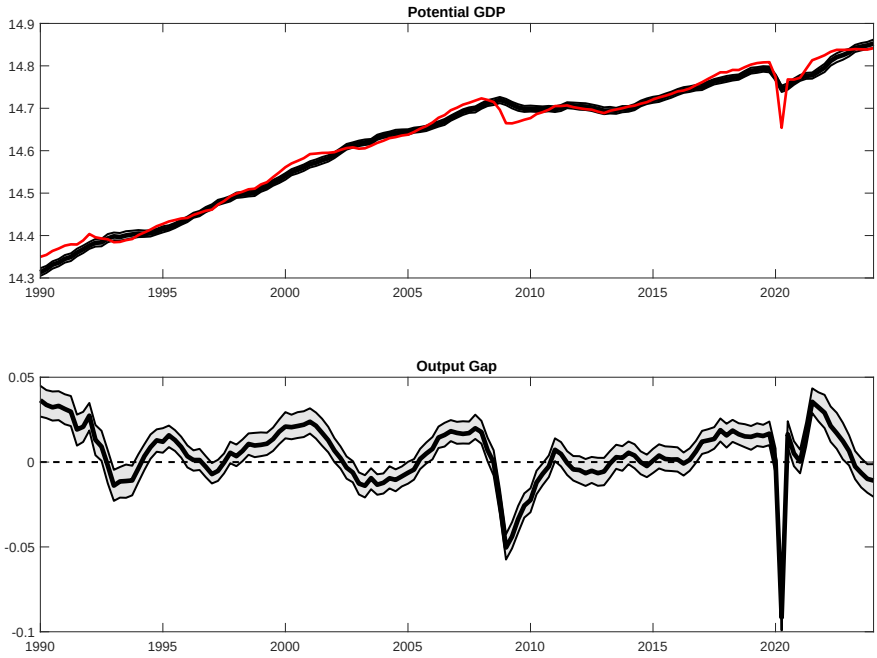

Figure 13. Actual data and estimated trends and cycles of real GDP in a model without Stochastic Volatility

Note: Point-wise median (solid black line) with 68% credible bands. Real GDP is defined in log terms. The model is estimated using the same priors but without the feature of Stochastic Volatility in both the permanent and transitory sides.

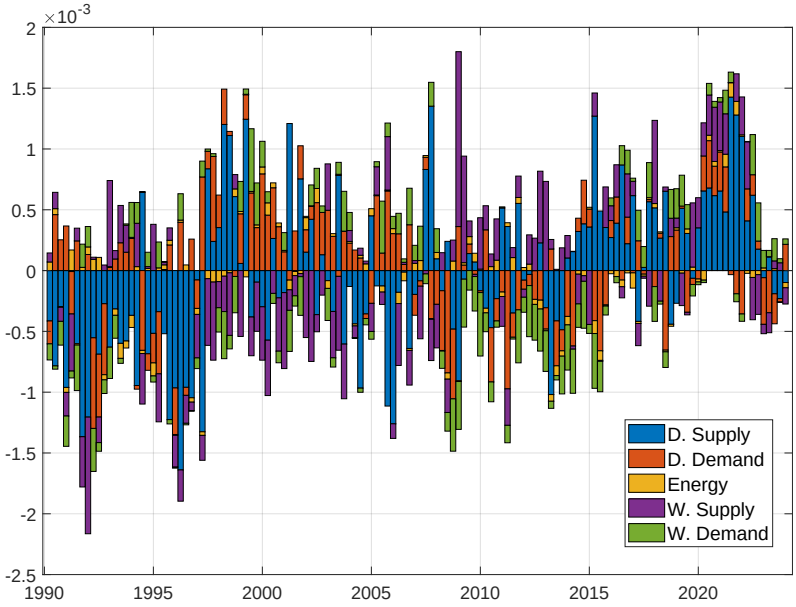

Figure 14. Estimated structural shocks of the point-wise median change of trend inflation from 1990Q2 to 2024Q1

Note: Colored bars depict the structural shocks —domestic (demand- and supply-side), global (demand- and supply-side), and energy supply— affecting the changes in the point-wise median of trend inflation, at time t.

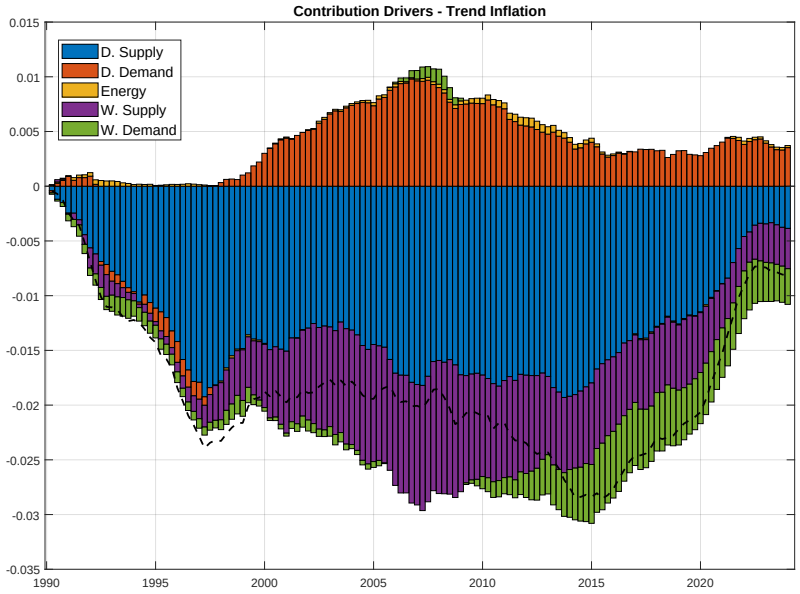

Figure 15. Estimated historical decomposition of the point-wise median of trend inflation from 1990Q2 to 2024Q1

Note: Both the black line, representing the point-wise median of trend inflation, and the colored bars, depicting the cumulative contribution of each structural shock—domestic (demand- and supply-side), global (demand- and supply-side), and energy supply—at time t, are expressed as deviations from the baseline period of 1990Q1.

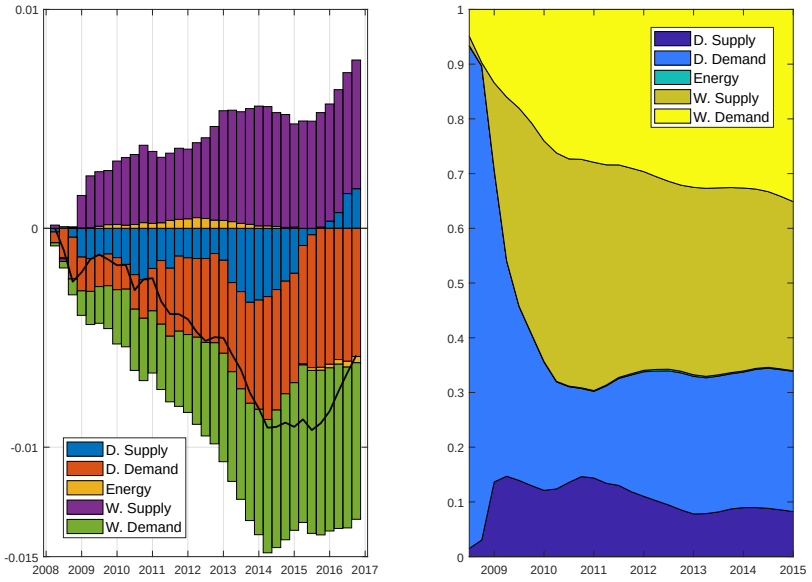

Figure 16. (Left) Estimated historical decomposition of the point-wise median of trend inflation (2008–2017). (Right) Relative percentage shares of structural shocks over the same period

Note: Left: The black line shows the point-wise median of trend inflation, and the colored bars show the cumulative contributions of each structural shock (domestic supply, domestic demand, global supply, global demand, and energy supply) at each date (t), all expressed as deviations from the 2008 Q1 baseline. Right: At each date, the shares are computed using a variance-decomposition–style normalization, so they sum to 100%, showing each shock's percentage share of the total change in trend inflation.

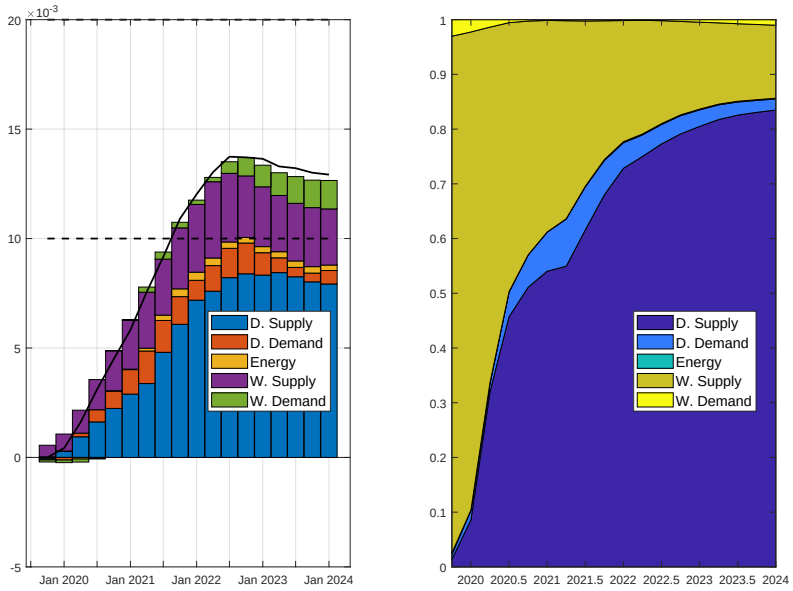

Figure 17. (Left) Estimated historical decomposition of the point-wise median of trend inflation (2020 to 2024). (Right) Relative percentage shares of structural shocks over the same period

Note: Left: The black line shows the point-wise median of trend inflation, and the colored bars show the cumulative contributions of each structural shock (domestic supply, domestic demand, global supply, global demand, and energy supply) at each date (t), all expressed as deviations from the 2019Q3 baseline. Right: At each date, the shares are computed using a variance-decomposition–style normalization, so they sum to 100%, showing each shock's percentage share of the total change in trend inflation.

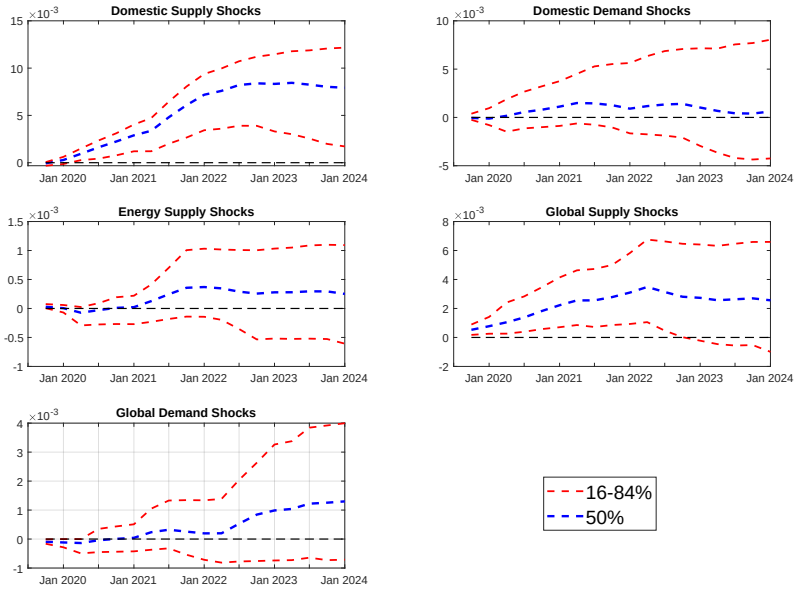

Figure 18. Posterior uncertainty for the estimated historical decomposition of trend inflation from 2020 to 2024

Note: The colored lines depict the cumulative contribution of each structural shock—domestic (demand- and supply-side), global (demand- and supply-side), and energy supply—at time t, expressed as deviations from the baseline period of 2019Q3. The colored blue lines represent the point-wise median contribution of each structural shock, while red lines represent the associated 68% confidence set.

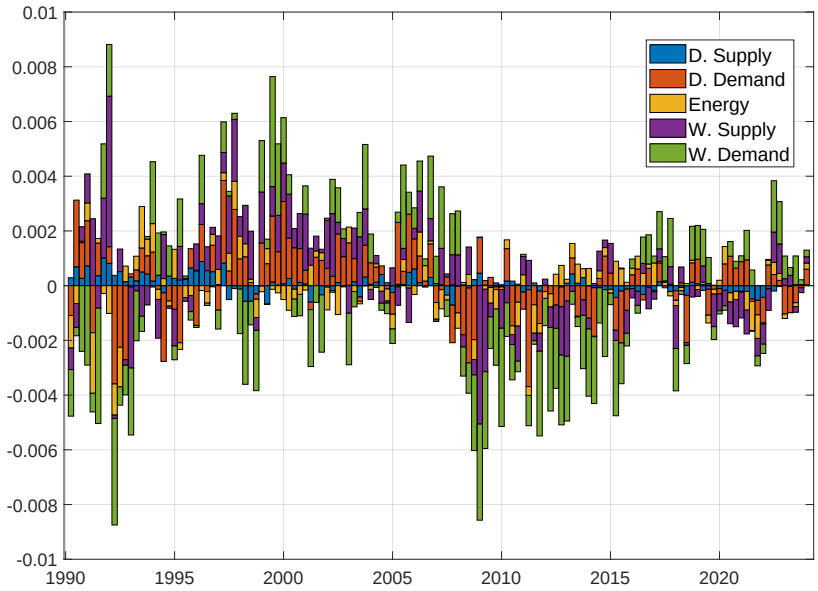

Figure 19. Estimated structural shocks of the point-wise median change of potential GDP, discounting the drift $\bar{c}$, from 1990Q2 to 2024Q1

Note: Colored bars depict the structural shocks —domestic (demand- and supply-side), global (demand- and supply-side), and energy supply— affecting the changes in the point-wise median of potential GDP, discounting the drift $\bar{c}$, at time t.

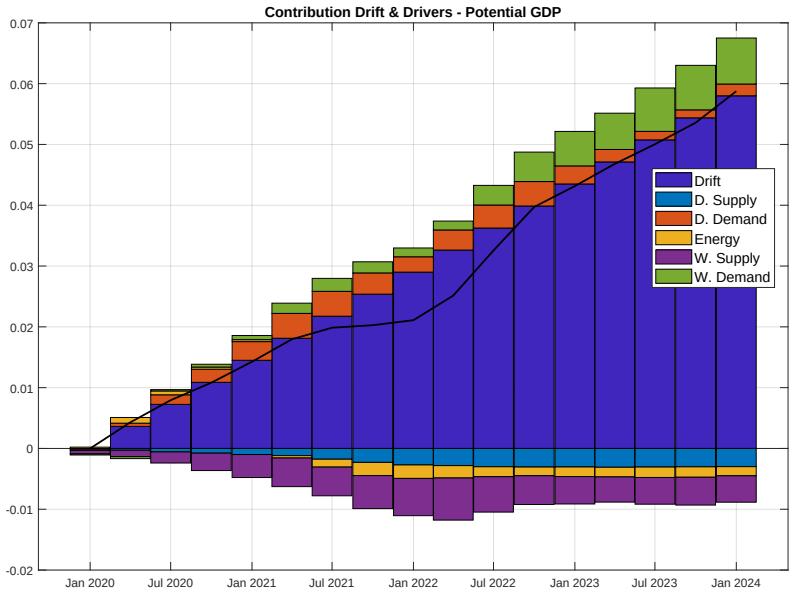

Figure 20. Cummulative contribution of the estimated drift and structural shocks of the point-wise median of potential GDP, from 2020Q1 to 2024Q1

Note: Colored bars depict the cumulative contribution at each date of the drift and structural shocks —domestic (demand- and supply-side), global (demand- and supply-side), and energy supply— affecting the point-wise median of potential GDP.

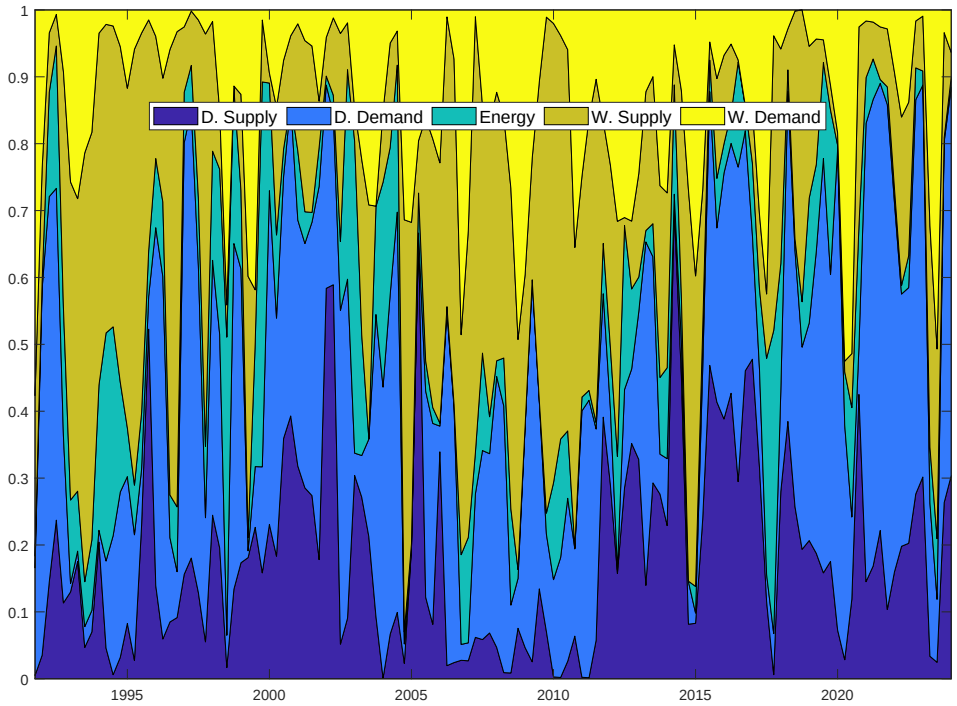

Figure 21. Relative shares of structural shocks for the historical decomposition of inflation-gap (point-wise median) over 1990Q2-2024Q1

Note: Colored areas show the percentage share of each structural shock—domestic supply, domestic demand, global supply, global demand, and energy supply—in the historical decomposition of the inflation-gap. At each date, the shares are computed using a variance-decomposition–style normalization, so they sum to 100%, highlighting each shock's relative importance.

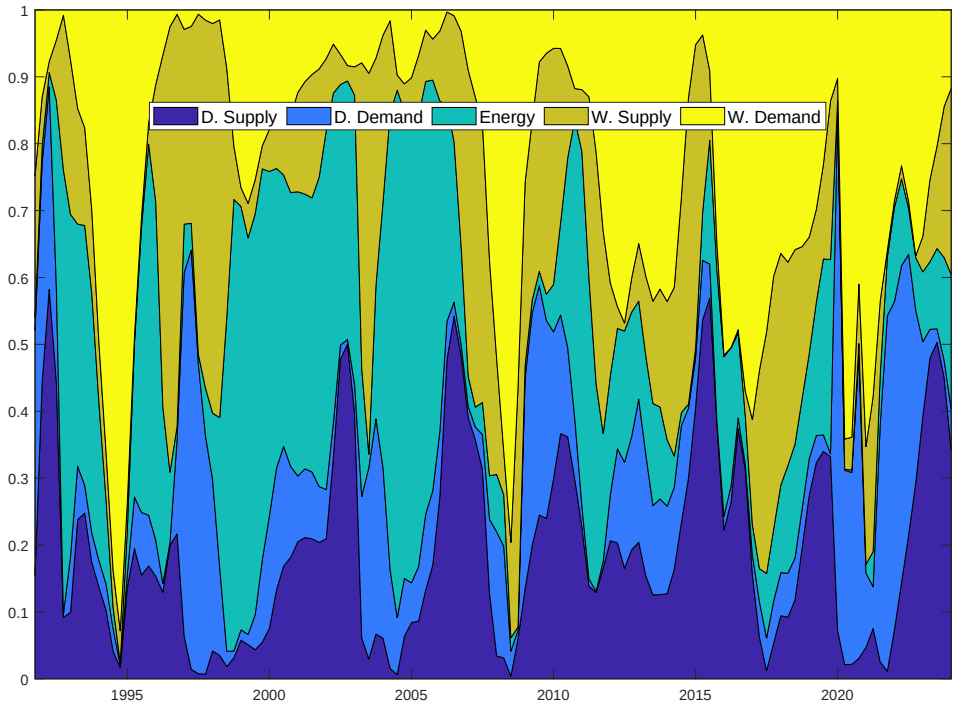

Figure 22. Relative shares of structural shocks for the historical decomposition of output-gap (point-wise median) over 1990Q2-2024Q1

Note: Colored areas show the percentage share of each structural shock—domestic supply, domestic demand, global supply, global demand, and energy supply—in the historical decomposition of the output-gap. At each date, the shares are computed using a variance-decomposition–style normalization, so they sum to 100%, highlighting each shock's relative importance.

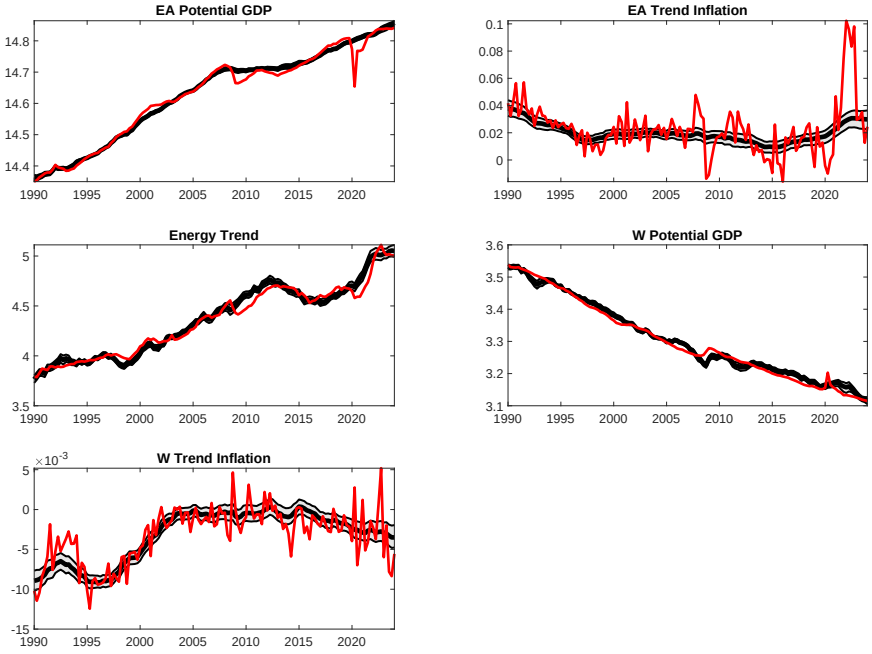

Figure 23. Actual data and estimated trends

Note: Point-wise median (solid black line) with 68% credible bands are based on 150000 draws. Variables are defined as in Table 1 and 2.

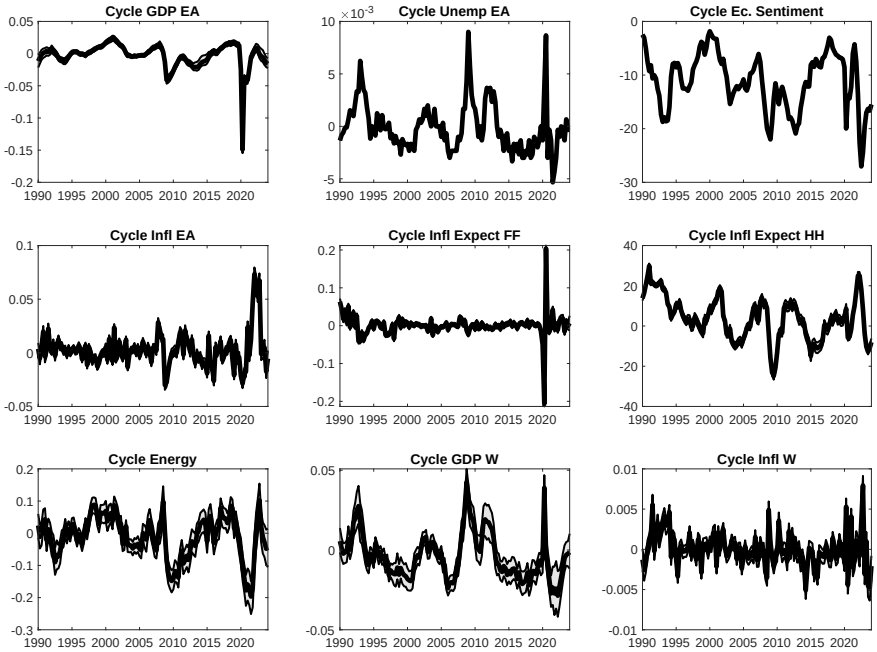

Figure 24. Actual data and estimated cycles

Note: Point-wise median (solid black line) with 68% credible bands are based on 150000 draws. Variables are defined as in Table 1 and 2.

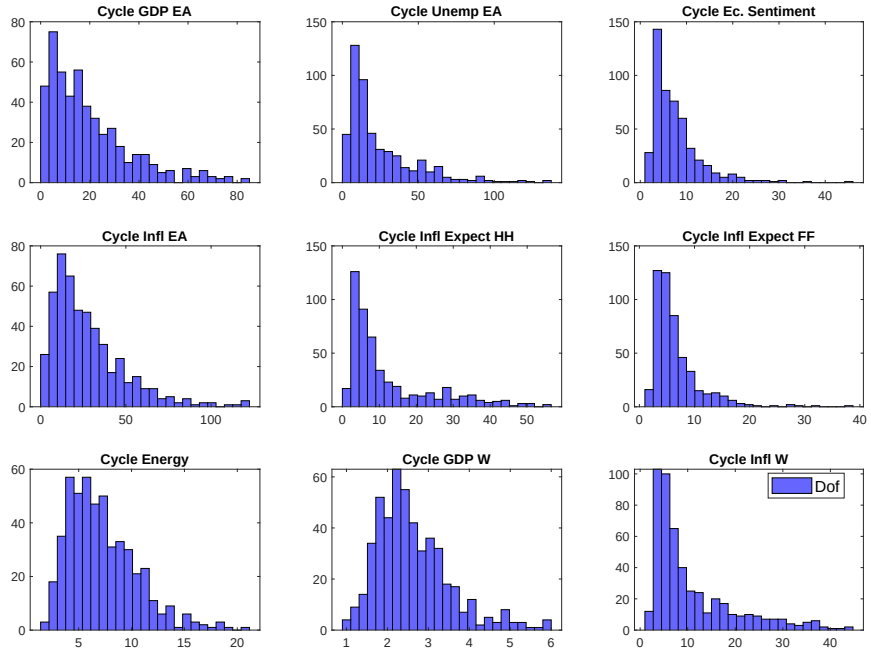

Figure 25. The posterior density of degrees of freedom (DOF) of each residual.

Note: The blue bars represent the frequency distribution of the DOF parameters from the model..

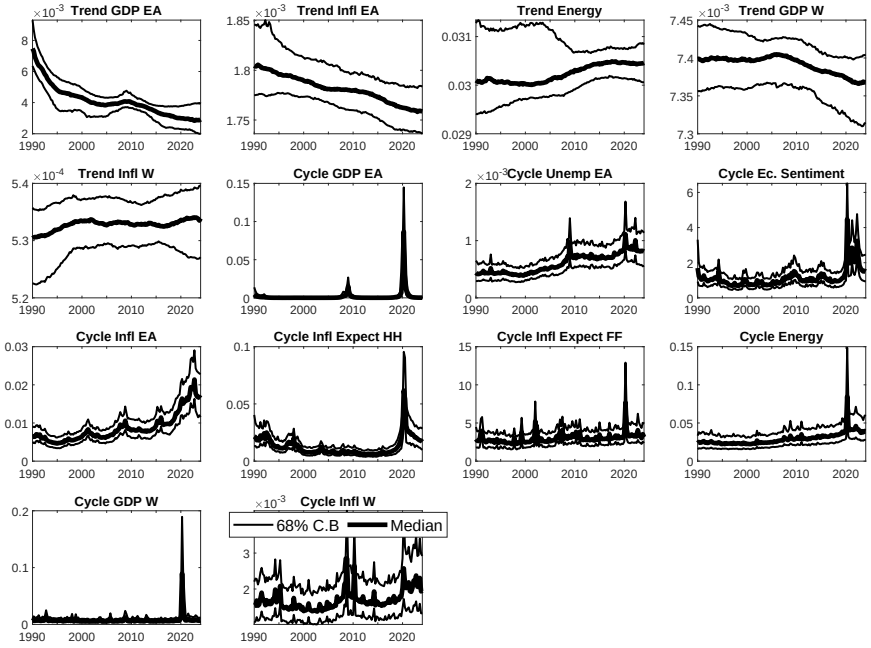

Figure 26. Stochastic volatility. The solid black lines are the posterior medians of the residual time-varing variances permanent (first five) and transitory (last nine), with 68% credible bands

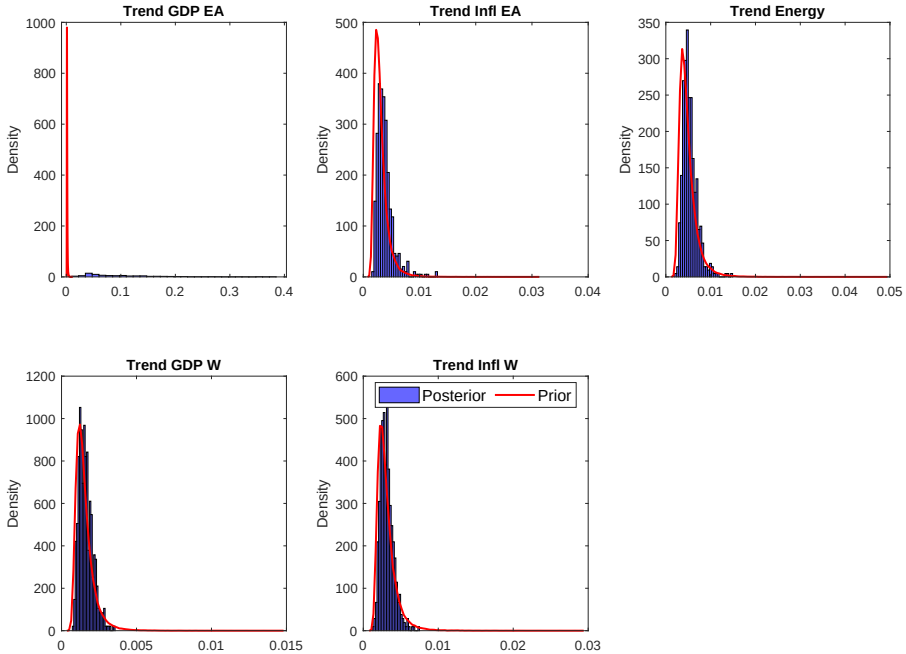

Figure 27. Prior and Posterior Densities of the Coefficients of G^{ϵ}

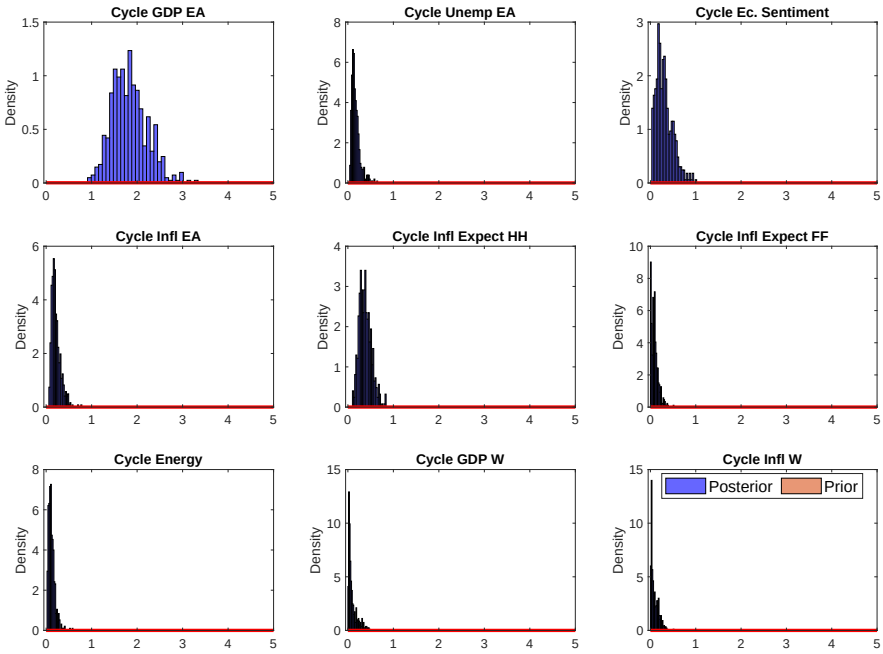

Figure 28. Prior and Posterior Densities of the Coefficients of G^u

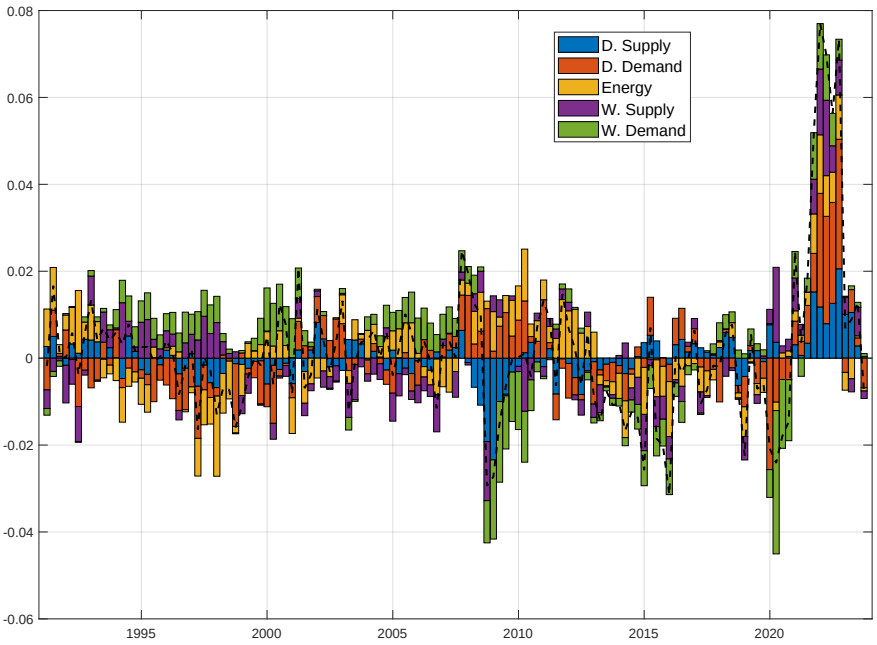

Figure 29. Historical decomposition of the point-wise median of inflation in deviations from its persistent component from 1991Q2 to 2024Q1. Estimated with a standard Bayesian VAR model

Note: The black line is the point-wise median of inflation in deviations from its persistent component. The colored bars represent the contribution of each structural shock—domestic (demand and supply-side), global (demand and supply-side), and energy supply—at time t.

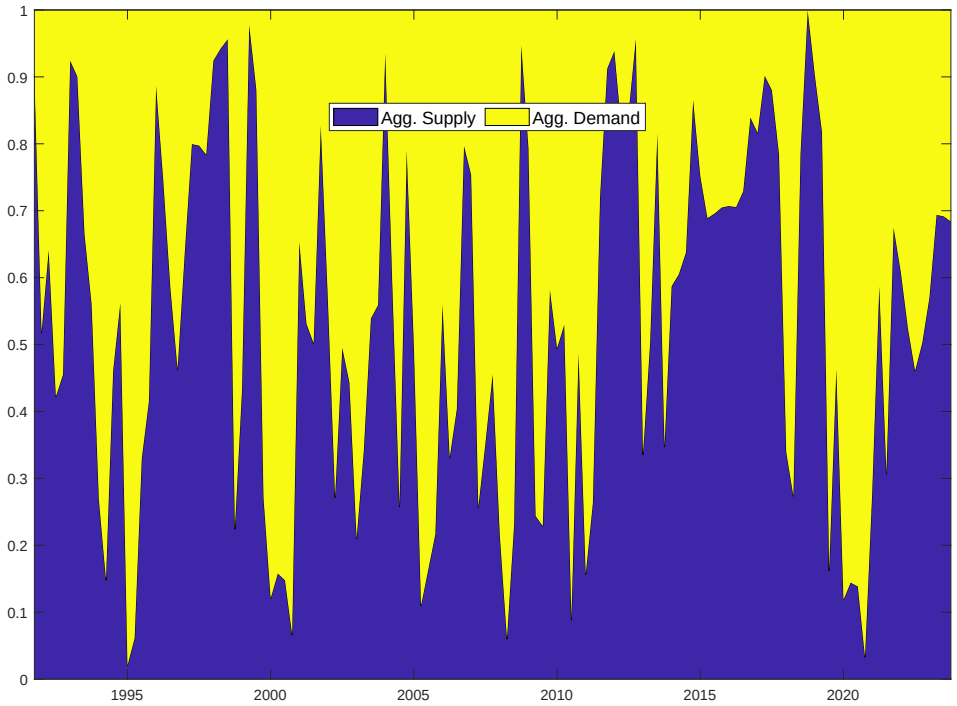

Figure 30. Relative shares of structural shocks for the historical decomposition of inflation-gap (point-wise median) over 1991Q2-2024Q1. Estimated with a standard Bayesian VAR model

Note: Colored areas show the percentage share of aggregate supply shocks—including domestic, global, and energy supply shocks—and aggregate demand shocks—including domestic, and global demand shocks—in the historical decomposition of the inflation in deviations from its persistent component. At each date, the shares are computed using a variance-decomposition–style normalization, so they sum to 100%, highlighting each shock's relative importance.

References

Abiad, Abdul, Prachi Mishra, and Petia Topalova, "How does trade evolve in the aftermath of financial crises?," *IMF Economic Review*, 2014, *62* (2), 213–247.

Alessandria, George, Joseph P Kaboski, and Virgiliu Midrigan, "Inventories, lumpy trade, and large devaluations," *American Economic Review*, 2010, *100* (5), 2304–2339.

Altissimo, Filippo, Michael Ehrmann, and Frank Smets, "Inflation persistence and price-setting behaviour in the Euro Area-a summary of the IPN evidence," *ECB Occasional paper*, 2006, (46).

Álvarez, Luis J and Mónica Correa-López, "Inflation expectations in euro area Phillips curves," *Economics Letters*, 2020, *195*, 109449.

Antolin-Diaz, Juan, Thomas Drechsel, and Ivan Petrella, "Tracking the slowdown in long-run GDP growth," *Review of Economics and Statistics*, 2017, *99* (2), 343–356.

Arce, Oscar, Matteo Ciccarelli, Antoine Kornprobst, and Carlos Montes-Galdón, "What caused the euro area post-pandemic inflation?," *ECB Occasional Paper*, 2024, (2024/343).

Arias, Jonas E, Juan F Rubio-Ramírez, and Daniel F Waggoner, "Inference based on structural vector autoregressions identified with sign and zero restrictions: Theory and applications," *Econometrica*, 2018, *86* (2), 685–720.

Arias, Jonas, Juan F Rubio-Ramirez, and Daniel F Waggoner, "Uniform priors for impulse responses," 2023.

Ascari, Guido and Luca Fosso, "The international dimension of trend inflation," *Journal of International Economics*, 2024, *148*, 103896.

_ , Dennis Bonam, and Andra Smadu, "Global supply chain pressures, inflation, and implications for monetary policy," *Journal of International Money and Finance*, 2024, *142*, 103029.

_ , _ , Lorenzo Mori, and Andra Smadu, "Fiscal Policy and Inflation in the Euro Area," 2024.

_ , Paolo Bonomolo, Marco Hoeberichts, and Riccardo Trezzi, *The euro area great inflation surge*, De Nederlandsche Bank nv, 2023.

Auer, Raphael, Claudio EV Borio, and Andrew J Filardo, "The globalisation of inflation: the growing importance of global value chains," 2017.

Baldwin, Richard E, *The great trade collapse: Causes, consequences and prospects*, Cepr, 2009.

Ball, Laurence, "Long-term damage from the Great Recession in OECD countries," *European Journal of Economics and Economic Policies*, 2014, *11* (2), 149–160.

Banbura, Marta, Elena Bobeica, and Catalina Martínez Hernández, "What drives core inflation? The role of supply shocks," 2023.

Barbarino, Alessandro, Travis J Berge, Han Chen, and Andrea Stella, "Which output gap estimates are stable in real time and why?," 2020.

Baumeister, Christiane and James D Hamilton, "Sign restrictions, structural vector autoregressions, and useful prior information," *Econometrica*, 2015, *83* (5), 1963–1999.

Bems, Rudolfs, Robert C Johnson, and Kei-Mu Yi, "The great trade collapse," *Annu. Rev. Econ.*, 2013, *5* (1), 375–400.

Bénassy-Quéré, Agnes, Giancarlo Corsetti, Antonio Fatás, Gabriel J FELBERMAYR, Marcel Fratzscher, Clemens Fuest, Francesco Giavazzi, Ramon Marimon, Philippe Martin, Jean Pisani-Ferry et al., "COVID-19 economic crisis: Europe needs more than one instrument," 2020.

Benati, Luca and Haroon Mumtaz, "US evolving macroeconomic dynamics: a structural investigation," 2007.

Benigno, Gianluca and Luca Fornaro, "Stagnation traps," *The Review of Economic Studies*, 2018, *85* (3), 1425–1470.

Bergholt, Drago, Fabio Canova, Francesco Furlanetto, Nicolò Maffei-Faccioli, and Pål Ulvedal, *What drives the recent surge in inflation? The historical decomposition roller coaster* number 7/2024, Working Paper, 2024.

_ , Francesco Furlanetto, and Etienne Vaccaro-Grange, "Did monetary policy kill the Phillips curve? Some simple arithmetics," *Review of Economics and Statistics*, 2024, pp. 1–45.

Beveridge, Stephen and Charles R Nelson, "A new approach to decomposition of economic time series into permanent and transitory components with particular attention to measurement of the 'business cycle'," *Journal of Monetary economics*, 1981, *7* (2), 151–174.

Bianchi, Francesco and Andrea Civelli, "Globalization and inflation: Evidence from a time-varying VAR," *Review of Economic Dynamics*, 2015, *18* (2), 406–433.

Blanchard, Olivier, Thomas Philippon, Jean Pisani-Ferry et al., *A new policy toolkit is needed as countries exit COVID-19 lockdowns*, JSTOR, 2020.

Bluedorn, Mr John C and Mr Daniel Leigh, *Hysteresis in labor Markets? Evidence from professional long-term forecasts*, International Monetary Fund, 2019.

Bobeica, Elena and Marek Jarociński, "Missing disinflation and missing inflation: A VAR perspective," *57th issue (March 2019) of the International Journal of Central Banking*, 2019.

_ **, Matteo Ciccarelli, and Isabel Vansteenkiste**, "The link between labor cost and price inflation in the euro area," 2019.

Bodnár, Katalin, Julien Le Roux, Paloma Lopez-Garcia, Béla Szörfi et al., "The impact of Covid-19 on potential output in the euro area," *Economic Bulletin Articles*, 2020, *7*.

Borio, Claudio EV and Andrew J Filardo, "Globalisation and inflation: New cross-country evidence on the global determinants of domestic inflation," 2007.

Bowles, Carlos, Roberta Friz, Veronique Genre, Geoff Kenny, Aidan Meyler, and Tuomas Rautanen, "The ECB survey of professional forecasters (SPF)-A review after eight years' experience," *ECB occasional paper*, 2007, (59).

Candia, Bernardo, Olivier Coibion, and Yuriy Gorodnichenko, "The Inflation Expectations of US Firms: Evidence from a new survey," Technical Report, National Bureau of Economic Research 2021.

Canova, Fabio and Gianni De Nicolo, "Monetary disturbances matter for business fluctuations in the G-7," *Journal of Monetary Economics*, 2002, *49* (6), 1131–1159.

Carriero, Andrea, Todd E Clark, Massimiliano Giuseppe Marcellino, and Elmar Mertens, "Addressing COVID-19 outliers in BVARs with stochastic volatility," 2021.

Carter, Chris K and Robert Kohn, "On Gibbs sampling for state space models," *Biometrika*, 1994, *81* (3), 541–553.

Chen, Ms Wenjie, Mr Mico Mrkaic, and Mr Malhar S Nabar, *The global economic recovery 10 years after the 2008 financial crisis*, International Monetary Fund, 2019.

Chiu, Ching-Wai Jeremy, Haroon Mumtaz, and Gabor Pinter, "Forecasting with VAR models: Fat tails and stochastic volatility," *International Journal of Forecasting*, 2017, *33* (4), 1124–1143.

Chor, Davin and Kalina Manova, "Off the cliff and back? Credit conditions and international trade during the global financial crisis," *Journal of international economics*, 2012, *87* (1), 117–133.

Ciccarelli, Matteo and Benoit Mojon, "Global inflation," *The Review of Economics and Statistics*, 2010, *92* (3), 524–535.

_ **and Juan Angel García**, "Expectation spillovers and the return of inflation," *Economics Letters*, 2021, *209*, 110119.

_ , **Chiara Osbat, Elena Bobeica, Caroline Jardet, Marek Jarocinski, Caterina Mendicino, Alessandro Notarpietro, Sergio Santoro, and Arnoud Stevens**, "Low inflation in the euro area: Causes and consequences," *ECB occasional paper*, 2017, (181).

Clark, Peter K, "The cyclical component of US economic activity," *The Quarterly Journal of Economics*, 1987, *102* (4), 797–814.

Clark, Todd E and Francesco Ravazzolo, "Macroeconomic forecasting performance under alternative specifications of time-varying volatility," *Journal of Applied Econometrics*, 2015, *30* (4), 551–575.

Cogley, Timothy and Thomas J Sargent, "Drifts and volatilities: monetary policies and outcomes in the post WWII US," *Review of Economic dynamics*, 2005, *8* (2), 262–302.

Coibion, Olivier and Yuriy Gorodnichenko, "Is the Phillips curve alive and well after all? Inflation expectations and the missing disinflation," *American Economic Journal: Macroeconomics*, 2015, *7* (1), 197–232.

Conti, Antonio Maria, Stefano Neri, and Andrea Nobili, "Low inflation and monetary policy in the euro area," *ECB Working Paper*, 2017.

Corsello, Francesco, Stefano Neri, and Alex Tagliabracci, "Anchored or de-anchored? That is the question," *European Journal of Political Economy*, 2021, *69*, 102031.

Corsetti, Giancarlo, Luca Dedola, and Sylvain Leduc, "The international dimension of productivity and demand shocks in the US economy," *Journal of the European Economic Association*, 2014, *12* (1), 153–176.

Croitorov, Olga, Giulia Filippeschi, Mirko Licchetta, Philipp Pfeiffer, Adriana Reut, Wouter Simons, Anna Thum-Thysen, Anneleen Vandeplas, and Lukas Vogel, "The macroeconomic impact of the COVID-19 pandemic in the euro area," *Q Rep Euro Area*, 2021, *20* (2), 7–16.

Cúrdia, Vasco, Marco Del Negro, and Daniel L Greenwald, "Rare shocks, great recessions," *Journal of Applied Econometrics*, 2014, *29* (7), 1031–1052.

Dao, Mai Chi, Pierre-Olivier Gourinchas, Daniel Leigh, and Prachi Mishra, "Understanding the international rise and fall of inflation since 2020," *Journal of Monetary Economics*, 2024, *148*, 103658.

Del Negro, Marco, Domenico Giannone, Marc P Giannoni, and Andrea Tambalotti, "Safety, liquidity, and the natural rate of interest," *Brookings Papers on Economic Activity*, 2017, *2017* (1), 235–316.

_ , _ , _ , **and** _ , "Global trends in interest rates," *Journal of International Economics*, 2019, *118*, 248–262.

Dovern, Jonas, Geoff Kenny et al., "Anchoring inflation expectations in unconventional times: Micro evidence for the euro area," *International Journal of Central Banking*, 2020, *16* (5), 309–347.

Duncan, Roberto and Enrique Martínez-García, "Forecasting inflation in open economies: What can a NOEM model do?," *Journal of Forecasting*, 2023, *42* (3), 481–513.

Eaton, Jonathan, Samuel Kortum, Brent Neiman, and John Romalis, "Trade and the global recession," *American Economic Review*, 2016, *106* (11), 3401–3438.

ECB, Staff, "Annual Report 2021," 2021.

_ , "Economic Bulletin Issue 8, 2022," 2022.

Fagan, Gabriel, Jerome Henry, and Ricardo Mestre, "An area-wide model for the euro area," *Economic Modelling*, 2005, *22* (1), 39–59.

Fernández-Villaverde, Jesús, Luis Garicano, and Tano Santos, "Political credit cycles: the case of the Eurozone," *Journal of Economic perspectives*, 2013, *27* (3), 145–166.

Ferroni, F and B Mojon, "Domestic and global drivers of inflation in the euro area," *ECB Economic Bulletin*, 2017, (4), 72–96.

Ferroni, Filippo and Benoit Mojon, "Domestic and global inflation," *Mimeo. Federal Reserve Bank of Chicago*, 2014.

Forbes, Kristin J, "Has globalization changed the inflation process?," 2019.

Fornaro, Luca and Martin Wolf, "The scars of supply shocks: Implications for monetary policy," *Journal of Monetary Economics*, 2023, *140*, S18–S36.

Foroni, Claudia, Francesco Furlanetto, and Antoine Lepetit, "Labor supply factors and economic fluctuations," *International Economic Review*, 2018, *59* (3), 1491–1510.

Furlanetto, Francesco, Antoine Lepetit, Ørjan Robstad, Juan Rubio-Ramírez, and Pål Ulvedal, "Estimating hysteresis effects," *American Economic Journal: Macroeconomics*, 2025, *17* (1), 35–70.

Galí, Jordi and Luca Gambetti, "On the sources of the great moderation," *American Economic Journal: Macroeconomics*, 2009, *1* (1), 26–57.

Geweke, John, "Bayesian treatment of the independent Student-t linear model," *Journal of applied econometrics*, 1993, *8* (S1), S19–S40.

_ , "Interpretation and inference in mixture models: Simple MCMC works," *Computational Statistics & Data Analysis*, 2007, *51* (7), 3529–3550.

Geweke, John F et al., "Evaluating the accuracy of sampling-based approaches to the calculation of posterior moments," Technical Report, Federal Reserve Bank of Minneapolis 1991.

Giannone, Domenico and G Primiceri, "Demand-driven inflation," Technical Report, Working paper. https://faculty. wcas. northwestern. edu/gep575 ... 2025.

_ **and Giorgio Primiceri**, "The drivers of post-pandemic inflation," Technical Report, National Bureau of Economic Research 2024.

_ **, Michele Lenza, and Giorgio E Primiceri**, "Prior selection for vector autoregressions," *Review of Economics and Statistics*, 2015, *97* (2), 436–451.

Gilje, Erik, Robert Ready, and Nikolai Roussanov, "Fracking, drilling, and asset pricing: Estimating the economic benefits of the shale revolution," Technical Report, National Bureau of Economic Research Cambridge, MA 2016.

Gimeno, Ricardo and Eva Ortega, "The evolution of inflation expectations in euro area markets," 2016.

Giordani, Paolo, Michael Pitt, and Robert Kohn, "Bayesian inference for time series state space models," 2011.

Gonçalves, Eduardo and Gerrit Koester, "The role of demand and supply in underlying inflation–decomposing HICPX inflation into components," *Economic Bulletin Boxes*, 2022, *7*.

González-Astudillo, Manuel and John M Roberts, "When are trend–cycle decompositions of GDP reliable?," *Empirical Economics*, 2022, *62* (5), 2417–2460.

Gordon, Robert J, "Inflation, flexible exchange rates, and the natural rate of unemployment," Technical Report, National Bureau of Economic Research 1981.

_ , "US inflation, labor's share, and the natural rate of unemployment," 1988.

_ , "The turtle's progress: Secular stagnation meets the headwinds," *Secular stagnation: facts, causes and cures*, 2014, pp. 47–59.

_ , "Secular stagnation: A supply-side view," *American economic review*, 2015, *105* (5), 54–59.

Gorter, Janko, Jan Jacobs, and Jakob De Haan, "Taylor rules for the ECB using expectations data," *Scandinavian Journal of Economics*, 2008, *110* (3), 473–488.

Guerrieri, Luca, Christopher Gust, and J David Lǿpez-Salido, "International competition and inflation: a New Keynesian perspective," *American Economic Journal: Macroeconomics*, 2010, *2* (4), 247–280.

Ha, Jongrim, M Ayhan Kose, and Franziska Ohnsorge, "Global inflation synchronization," 2019.

Harvey, Andrew C, "Trends and cycles in macroeconomic time series," *Journal of Business & Economic Statistics*, 1985, *3* (3), 216–227.

Hasenzagl, Thomas, Filippo Pellegrino, Lucrezia Reichlin, and Giovanni Ricco, "A Model of the Fed's View on Inflation," *The Review of Economics and Statistics*, 2018, pp. 1–45.

Hausman, Catherine and Ryan Kellogg, "Welfare and distributional implications of shale gas," Technical Report, National Bureau of Economic Research 2015.

Henriksen, Espen, Finn E Kydland, and Roman Šustek, "Globally correlated nominal fluctuations," *Journal of Monetary Economics*, 2013, *60* (6), 613–631.

Higgins, Matthew, Thomas Klitgaard et al., "How Much Have Consumers Spent on Imports during the Pandemic?," Technical Report, Federal Reserve Bank of New York 2021.

Hilscher, Jens, Alon Raviv, and Ricardo Reis, "How likely is an inflation disaster?," 2022.

IMF, "Global disinflation in an era of constrained monetary policy," *World Economic Outlook*, 2016.

_ , "Recent wage dynamics in advanced economies: Drivers and implications," *World Economic Outlook, October 2017: Seeking sustainable growth: Short-term recovery, long-term challenges*, 2017, pp. 73–112.

Inoue, Atsushi and Lutz Kilian, "Joint Bayesian inference about impulse responses in VAR models," *Journal of Econometrics*, 2022, *231* (2), 457–476.

Jacquier, Eric, Nicholas G Polson, and Peter E Rossi, "Bayesian analysis of stochastic volatility models with fat-tails and correlated errors," *Journal of Econometrics*, 2004, *122* (1), 185–212.

Jarociński, Marek and Michele Lenza, "An inflation-predicting measure of the output gap in the euro area," *Journal of Money, Credit and Banking*, 2018, *50* (6), 1189–1224.

Johannsen, Benjamin K and Elmar Mertens, "A Time-Series Model of Interest Rates with the Effective Lower Bound," *Journal of Money, Credit and Banking*, 2021, *53* (5), 1005–1046.

Kabukçuoğlu, Ayşe and Enrique Martínez-García, "Inflation as a global phenomenon—Some implications for inflation modeling and forecasting," *Journal of Economic Dynamics and Control*, 2018, *87*, 46–73.

Kamber, Güneş, James Morley, and Benjamin Wong, "Intuitive and reliable estimates of the output gap from a Beveridge-Nelson filter," *Review of Economics and Statistics*, 2018, *100* (3), 550–566.

_ , _ , **and** _ , "Trend-cycle decomposition in the presence of large shocks," *Journal of Economic Dynamics and Control*, 2025, p. 105066.

Kilian, Lutz, "The economic effects of energy price shocks," *Journal of economic literature*, 2008, *46* (4), 871–909.

_ , "Not all oil price shocks are alike: Disentangling demand and supply shocks in the crude oil market," *American Economic Review*, 2009, *99* (3), 1053–69.

Koester, Gerrit, Jakob Nordeman, Michel Soudan et al., "Comparing recent inflation developments in the United States and the euro area," *Economic Bulletin Boxes*, 2021, *6.*

_ **, Sofia Cuquerella Ricarte, Ramon Gomez-Salvador et al.**, "Recent inflation developments in the United States and the euro area–an update," *Economic Bulletin Boxes*, 2022, *1.*

Laxton, Douglas and Robert Tetlow, *A simple multivariate filter for the measurement of potential output*, Vol. 59, Bank of Canada Technical Report No. 59. Ottawa, 1992.

Lenza, Michele and Giorgio E Primiceri, "How to estimate a vector autoregression after march 2020," *Journal of Applied Econometrics*, 2022.

Levchenko, Andrei A, Logan T Lewis, and Linda L Tesar, "The collapse of international trade during the 2008-2009 crisis: In search of the smoking gun," Technical Report, National Bureau of Economic Research 2010.

Łyziak, Tomasz and Maritta Paloviita, "Anchoring of inflation expectations in the euro area: recent evidence based on survey data," *European Journal of Political Economy*, 2017, *46*, 52–73.

Maffei-Faccioli, Nicolò, "Identifying the sources of the slowdown in growth: Demand versus supply," *Journal of Applied Econometrics*, 2025.

Martin, Fernando M, Juan M Sánchez, and Olivia Wilkinson, "The economic impact of COVID-19 around the world," *FRB St. Louis Working Paper*, 2022, (2022-30).

Martínez-García, E and MA Wynne, *The global slack hypothesis* number 10, DIANE Publishing, 2010.

Morley, James and Benjamin Wong, "Estimating and accounting for the output gap with large Bayesian vector autoregressions," *Journal of Applied Econometrics*, 2020, *35* (1), 1–18.

_ **, Trung Duc Tran, and Benjamin Wong**, "A simple correction for misspecification in trend-cycle decompositions with an application to estimating r," *Journal of Business & Economic Statistics*, 2024, *42* (2), 665–680.

Muggenthaler, Philip, Joachim Schroth, and Yiqiao Sun, "The heterogeneous economic impact of the pandemic across euro area countries," *Economic Bulletin Boxes*, 2021, *5*.

Mumtaz, Haroon and Paolo Surico, "Evolving international inflation dynamics: world and country-specific factors," *Journal of the European Economic Association*, 2012, *10* (4), 716–734.

O'Brien, Derry, Clemence Dumoncel, Eduardo Goncalves et al., "The role of demand and supply factors in HICP inflation during the COVID-19 pandemic–a disaggregated perspective," *Economic Bulletin Articles*, 2021, *1*.

Peersman, Gert and Ine Van Robays, "Oil and the Euro area economy," *Economic Policy*, 2009, *24* (60), 603–651.

Primiceri, Giorgio E, "Time varying structural vector autoregressions and monetary policy," *The Review of Economic Studies*, 2005, *72* (3), 821–852.

Rubio-Ramirez, Juan F, Daniel F Waggoner, and Tao Zha, "Structural vector autoregressions: Theory of identification and algorithms for inference," *The Review of Economic Studies*, 2010, *77* (2), 665–696.

Santis, Roberto A De, "Supply chain disruption and energy supply shocks: impact on euro area output and prices," 2024.

_ **and Grigor Stoevsky**, "The role of supply and demand in the post-pandemic recovery in the euro area," *Economic Bulletin Articles*, 2023, *4*.

Schorfheide, Frank and Dongho Song, "Real-time forecasting with a (standard) mixed-frequency VAR during a pandemic," Technical Report, National Bureau of Economic Research 2021.

Stephens, Matthew, "Dealing with label switching in mixture models," *Journal of the Royal Statistical Society: Series B (Statistical Methodology)*, 2000, *62* (4), 795–809.

Stock, James H and Mark W Watson, "Variable trends in economic time series," *Journal of economic perspectives*, 1988, *2* (3), 147–174.

_ **and** _ , "Why has US inflation become harder to forecast?," *Journal of Money, Credit and banking*, 2007, *39*, 3–33.

Strohsal, Till and Lars Winkelmann, "Assessing the anchoring of inflation expectations," *Journal of International Money and Finance*, 2015, *50*, 33–48.

Summers, Lawrence H, "U.S. Economic Prospects: Secular Stagnation, Hysteresis, and the Zero Lower Bound," *Business Economics*, 2014, pp. 65–73.

Uhlig, Harald, "What are the effects of monetary policy on output? Results from an agnostic identification procedure," *Journal of Monetary Economics*, 2005, *52* (2), 381–419.

Watson, Mark W, "Univariate detrending methods with stochastic trends," *Journal of monetary economics*, 1986, *18* (1), 49–75.

Wolf, Christian K, "Svar (mis) identification and the real effects of monetary policy shocks," *American Economic Journal: Macroeconomics*, 2020, *12* (4), 1–32.

_ , "What can we learn from sign-restricted VARs?," in "AEA Papers and Proceedings," Vol. 112 American Economic Association 2014 Broadway, Suite 305, Nashville, TN 37203 2022, pp. 471–475.

Yellen, Janet, "Macroeconomic Research After the Crisis: a speech at\" The Elusive'Great'Recovery: Causes and Implications for Future Business Cycle Dynamics\" 60th annual economic conference sponsored by the Federal Reserve Bank of Boston, Boston, Massachusetts, October 14, 2016," Technical Report, Board of Governors of the Federal Reserve System (US) 2016.